Synthetic seismicity scenarios to inform large earthquake emergency response in the greater North Island, New Zealand, with specific attention to events that severely impact the Wellington region

Fry B, JL Hayes, C Penney, NA Horspool
AE Kaiser, A Nicol, M Liao, A Howell
CI Massey, B Lukovic, S Inglis, WL Power
DR Burbidge, AR Gusman, X Wang, MA Clive
DH Charlton, KKS Thingbaijam, C DiCaprio

GNS Science Consultancy Report 2022/115
March 2023 – Revised

BIBLIOGRAPHIC REFERENCE

Fry B, Hayes JL, Penney C, Horspool NA, Kaiser AE, Nicol A, Liao M, Howell A, Massey CI, Lukovic B, et al. 2023. Synthetic seismicity scenarios to inform large earthquake emergency response in the greater North Island, New Zealand, with specific attention to events that severely impact the Wellington region. Lower Hutt (NZ): GNS Science. 58 p. Consultancy Report 2022/115. Revised March 2023.

CONTENTS

FIGURES

APPENDICES

APPENDIX FIGURES

APPENDIX TABLES

EXECUTIVE SUMMARY

We use a recently created computational catalogue of synthetic earthquakes in New Zealand to investigate complicated earthquake sequences that could severely impact the Wellington region. The catalogue contains over 300,000 years' worth of simulated earthquake scenarios. Using computational models allows us to investigate complex potential earthquakes that are not represented in the historical record and are difficult or impossible to account for with traditional seismic hazard approaches. We select 10 scenarios from our catalogue that could severely impact Wellington. These scenarios were chosen because they represent suites of events, with multiple other similar scenarios occurring in the catalogue. We assess each scenario for impacts to Wellington, Palmerston North and Auckland. We note that this assessment represents a bulk summary at a regional scale and is not intended to be, nor suitable for, detailed site assessment. For each of the scenarios, we estimate the broad potential for (1) damaging ground motion, (2) significant risk of landslides and (3) tsunami inundation. Owing largely to the proximity of Wellington and Palmerston North, four of the ten considered representative scenarios have severe impacts in both of these cities, while another four have at least moderate impacts in both cities. It is our opinion that many possible events that will significantly damage Wellington also have the potential to significantly damage Palmerston North. Only one of the considered scenarios, a full rupture of the Hikurangi Margin in an M9.1 earthquake, would be likely to generate at least moderate impacts in both Wellington and Auckland. However, significant uncertainty in ground motion for the Auckland region exists in this and similar scenarios and should be the focus of additional research efforts to understand the range of credible risks posed to Auckland from such an event. We also highlight uncertainties around the impact of an Alpine Fault rupture on North Island faults. Ongoing National Science Challenge work is aimed at understanding the possibility of multi-fault rupture of the Alpine and Marlborough faults across Cook Strait, including North Island faults. Additionally, further work is needed to ensure that these computational models are consistent with understandings of potential complex earthquakes from other data sources and represent our best understanding of how earthquake-generating faults interact.

1.0 INTRODUCTION

The past two decades of earthquakes in New Zealand have taught us a grave and fundamental lesson: traditional scenario-driven approaches to emergency-response planning will likely fail to anticipate the complexity of hazards in the next large earthquake. This is largely because the historical record of earthquakes is short compared to geological timescales and paleoseismology information is insufficient to provide a complete picture of complicated earthquakes. Recent earthquakes in New Zealand highlight the gap between expectations of the complexity and severity of future earthquakes and reality.

For example, the 2009 M_W 7.9 Dusky Sound earthquake triggered a surprisingly large number of earthquake-induced landslides, generated surprisingly little high-frequency and abundant low-frequency ground motion (Fry et al. 2010) and affected long-term seismicity patterns as far away as the Canterbury Plains (Yin et al. 2021). The 2011 M_W 7.1 Darfield earthquake ruptured numerous faults that would not have been anticipated to rupture together in the same event based on traditional approaches to seismic hazard modelling (Gledhill et al. 2011) and ultimately triggered the M_W 6.2 Christchurch earthquake (Kaiser et al. 2012). The 2016 M_W 7.8 Kaikōura earthquake is widely accepted to be one of the most complex multi-fault earthquakes ever recorded (Kaiser et al. 2017) and triggered earthquakes across most of the North Island (Peng et al. 2018; Yao et al. 2021). How do we prepare for the ‘next big event’ when this will almost certainly contain features that we have never seen before? These features, for example, might be the spatial distribution of strong ground shaking, the likelihood of widespread landsliding or liquefaction or the role of other faults at regional distances to become part of the earthquake sequence.

Commonly, stress-testing of emergency-response systems is accomplished through the development of key scenarios by panels of experts followed by simulated response to those scenarios. Physics-based earthquake simulators have the potential to add value to this process by highlighting scenarios that have not yet been observed or considered. These simulators generate sets of synthetic potential earthquakes, based on our current understandings of earthquake physics and active fault systems in Aotearoa New Zealand, which can then be combined with modelling of secondary hazards, such as landslides or tsunami. These types of simulators have passed plausibility tests overseas (e.g. Richards-Dinger and Dieterich 2012; Shaw et al. 2018) and in New Zealand (Robinson and Benites 1996; Shaw et al. 2022) and are currently undergoing further testing and validation within the Resilience to Nature’s Challenges [RNC] National Science Challenge RNC2 programme.

This report outlines some scenarios that have the potential to have widespread impacts in the North Island. These are mostly focused on multi-fault ruptures – the type of earthquake that is most difficult to explore in the National Seismic Hazard Model (NSHM). In particular, we give examples of earthquakes involving both the Hikurangi subduction interface and shallower faults in the North Island. A significant complication of the models is to understand the nature of the complex and widespread triggering we see during the largest scenarios in the model. While the triggering shown in this report represents cosesimic failure of secondary faults, we still have work ahead to understand the role of early aftershocks in the scenarios (i.e. do some of the triggered faults more likely fail during aftershock sequences). This is especially true of the largest event show, the full margin M9.1 Hikurangi event. But, for the purposes of event response planning, the benefits far outweigh the challenges, as they provide us with the insight that regions distant to the primary rupture may experience damaging ground shaking during or shortly after the main event. We note that the scope of this report includes a regional-scale assessment of the severity of scenario events. The scope in no way intends or is suited to replace a detailed site assessment for local-scale impacts of the scenarios.

Using results from the simulators comes with challenges, including assigning return rates (likelihoods) to the events in the catalogue. Quite simply, earthquake simulators are too new to have undergone the level of rigorous testing that traditional source models for seismic hazard have. We have therefore queried the NSHM for bulk hazard information relating to the scenarios presented. In Appendix 3, we present return periods of suites of events with similar characteristics (magnitude and gross geographic location) to the events presented in this report. We believe that this hybrid physical and statistical approach reaps the benefits of both techniques by utilising physical knowledge of the earthquake process and by capitalising on the statistical power of probabilistic modelling.

2.0 APPROACH

In this report, we present an alternative method to create response scenarios that affect the Wellington region, and then we examine their impacts on two other key areas, Palmerston North and Auckland. The reason for choosing these regions is to inform a screening process and identify the possible consequences at a regional level to the National Crisis Management Centre (NCMC) and potential alternate National Crisis Management Centres (aNCMCs). By using knowledge of the *way* that earthquakes happen from laboratory experiments, we have developed an approximately 300 kyr record of about a million possible earthquakes in New Zealand (synthetic seismicity catalogue of the RNC National Science Challenge published in Shaw et al. [2022]). We believe that this synthetic catalogue highlights some of the complex earthquakes (or earthquake sequences) that may pose significant cascading and broadly reaching hazards for New Zealand. In this catalogue, we see striking complexity in the largest earthquakes. This complexity happens often and is consistent with the complexity of the very limited observations of events recorded in New Zealand over the last two decades. Using synthetic catalogues to generate scenarios for response system stress-testing is not only insightful but also necessary to consider the wealth of variation in natural stochastic earthquake systems.

We have chosen the scenarios to represent suites of similar events that recur in the catalogue. For each of the 10 chosen scenarios, we assess the shaking, landslide and tsunami hazard of each earthquake. Shaking assessment is conducted with the application of ground-motion prediction equations within the OpenQuake framework (Appendix 2), and results for the dominant and secondary faults of each scenario are combined to make a single model of ground motion, noting that the secondary faults may be treated as either coseismic or early aftershocks. Ground motions are subsequently converted to instrumental intensity. We apply a threshold of MMI7+ to characterise shaking as severe, MMI5–6 as moderate and MMI4–1 as minor (see Figures 3.1 and 3.2). Landslide assessment is based on the spatial distribution of calculated ground motions. Under the probabilistic landslide framework developed in the Earthquake-Induced Landslide Dynamics (EILD) Endeavour programme, the density of landslides triggered by the earthquake shaking is calculated for each element of a geotechnical spatial model of New Zealand (Appendix 3). We apply a quartile ranking for coseismic landslide hazard (Appendix 4), with 1 being low (Figures 3.1 and 3.2) and 4 being high (Figures 3.1 and 3.2). We finally qualitatively assess the tsunami potential for each of the scenarios and regions of interest through an expert elicitation process to develop the summary table presented in Section 3. We assess for both possibility of land inundation at critical sites and coastal tsunami amplitudes of ≥1 m, the threshold for triggering land threat. We also summarise relevant information from the existing probabilistic tsunami hazard model for New Zealand in Appendix 5.

3.0 RESULTS

We graphically summarise the event peril-specific results in Figure 3.1 and consolidate the results to represent city-specific hazards in Figure 3.2. Owing largely to shaking impacts, at least four of the ten scenarios we consider pose significant risk to both Wellington and Palmerston North, while an additional four have a moderate potential to significantly affect both Wellington and Palmerston North. Only one of the ten considered scenarios (a full margin, M_W 9.1 rupture of the Hikurangi megathrust) poses significant risk to both Wellington and Auckland. We note that significant uncertainty surrounds the estimation of strong ground shaking for Auckland in this event, and further work is suggested to better assess the ground-shaking impacts of this and similar scenarios. At present, this work cannot provide a formal likelihood of this or similar events. This or similar scenarios involving rupture of most of the Hikurangi Margin with M8–M9 happen in our catalogue every few hundred years with a most common recurrence interval of about 1000 years for the very largest (M9+) events (see Appendix 1, Figure A1.2). We present a detailed analysis of comparison with the NSHM in Appendix 3, in which we list inter-event intervals for similar magnitude earthquakes (albeit physically simpler) in the 2022 NSHM.

aNCMC Summary Results

		1 - Alpine Fault and Wairau	2 - Full Hikurangi and upper crustal faults	3 - Southern Hikurangi and Wellington Region faults (A)	4 - Southern Hikurangi and Wellington Region faults (B)	5 - Southern Hikurangi	6 - Western offshore faults (Mascarin)	7 - Fisherman's Fault	8 - Northern Ohariu Fault	9 - Northern Wairarapa Fault	10 - Aotea-Evan's Bay Fault
		7.7 Mw	9.1 Mw	8.5 Mw	8.4 Mw	8.9 Mw	7.2 Mw	7.2 Mw	6.9 Mw	7.1 Mw	6.5 Mw
BEEHIVE	**Expected ground shaking (MMI)**	MMI 7	MMI 9	MMI 9	MMI 9	MMI 9	MMI 5	MMI 7	MMI 5	MMI 6	MMI 9
	Density of coseismic landslides	3 - high	4 - very high	4 - very high	4 - very high	4 - very high	3 - high	3 - high	3 - high	3 - high	4 - very high
	Likelihood of exceeding severe shaking (MMI 7)	likely	highly likely	highly likely	highly likely	highly likely	unlikely	likely	unlikely	unlikely	highly likely
	Likelihood of exceeding very high landslide density	highly likely	highly likely	highly likely	highly likely	highly likely	likely	highly likely	likely	likely	likely
	Likelihood of flooding in Bowen House ground floor *(Beehive basement proxy)*	highly unlikely	highly likely	unlikely	unlikely	highly likely (-)	highly unlikely	highly unlikely	highly unlikely	highly unlikely	highly unlikely
WELLINGTON	**Expected ground shaking (MMI)**	MMI 7	MMI 9	MMI 9	MMI 9	MMI 9	MMI 5	MMI 7	MMI 5	MMI 6	MMI 9
	Density of coseismic landslides	3 - high	4 - very high	4 - very high	4 - very high	4 - very high	3 - high	3 - high	3 - high	3 - high	4 - very high
	Likelihood of severe shaking (MMI7)	likely	highly likely	highly likely	highly likely	highly likely	unlikely	likely	unlikely	unlikely	highly likely
	Likelihood of exceeding very high landslide density	highly likely	highly likely	highly likely	highly likely	highly likely	likely	highly likely	likely	likely	likely
	Likelihood of >1m coastal inundation	likely (+)	highly likely	highly likely	highly likely	highly likely	highly likely	highly likely	unlikely	unlikely	likely
PALMERSTON NORTH	**Expected ground shaking (MMI)**	MMI5	MMI9	MMI9	MMI8	MMI9	MMI6	MMI6	MMI7	MMI6	MMI4
	Density of coseismic landslides	1 - low	4 - very high	4 - very high	3 - high	4 - very high	1 - low	1 - low	1 - low	1 - low	1 - low
	Likelihood of severe shaking (MMI7)	unlikely	highly likely	highly likely	highly likely	highly likely	unlikely	unlikely	likely	unlikely	highly likely
	Likelihood of exceeding very high landslide density	likely	highly likely	likely	highly likely	highly likely	likely	likely	likely	likely	highly likely
	Likelihood of flooding at Manawatu alternative sites	highly unlikely	highly unlikely	highly unlikely	highly unlikely	highly unlikely	highly unlikely	highly unlikely	highly unlikely	highly unlikely	highly unlikely
AUCKLAND	**Expected ground shaking (MMI)**	MMI 1	MMI 5	MMI 2/3	MMI 2/3	MMI 4/5	MMI 2/3	MMI 1	MMI 1	MMI 1	MMI 1
	Density of coseismic landslides	1 - low	1 - low	1 - low	1 - low	1 - low	1 - low	1 - low	1 - low	1 - low	1 - low
	Likelihood of severe shaking (MMI7)	highly unlikely	unlikely	highly unlikely	highly unlikely	unlikely	highly unlikely	highly unlikely	highly unlikely	highly unlikely	highly unlikely
	Likelihood of exceeding very high landslide density	likely	likely	likely	likely	likely	unlikely	highly unlikely	highly unlikely	highly unlikely	highly unlikely
	Likelihood >1m coastal inundation in Auckland region	highly unlikely	highly likely	unlikely	unlikely	likely	highly unlikely	highly unlikely	highly unlikely	highly unlikely	highly unlikely
	Likelihood of flooding at Auckland alternative sites	highly unlikely	highly unlikely	highly unlikely	highly unlikely	highly unlikely	highly unlikely	highly unlikely	highly unlikely	highly unlikely	highly unlikely

Legend

Likelihood	highly unlikely	unlikely	likely	highly likely	
Expected ground shaking (MMI)	Intensity of ground shaking as defined in the Modified Mercalli Intensity Scale				
	MMI 1-2	MMI 3-4	MMI 5-6	MMI 7-8	MMI 9
Density of coseismic landslides	Volume (or area) of landsliding produced by shaking in the earthquake scenarios				
	1 - Low	2 - Mod	3 - High	4 - V. high	
Likelihood of severe shaking (MMI7)	Qualitative likelihood of Very Strong shaking, above which some buildings and infrastructure may expect damage				
Likelihood of exceeding very high landslide density	Qualitative likelihood of landsliding above which historical evidence has shown us to be significantly disruptive				
Likelihood >1m coastal inundation in Auckland region	Qualitative likelihood of tsunami waves sufficient to support evacuation of prone coastal regions				
Likelihood of flooding at Auckland alternative sites	Qualitative likelihood of tsunami inundation at proposed alternative sites.				

Figure 3.1 Summary table of scenario-dependent hazard for Wellington, Palmerston North and Auckland.

Scenario #	Name	Mw	Wellington	Palmerston North	Auckland
1	**Alpine Fault and Wairau**	7.7			
2	**Full Hikurangi and upper crustal faults**	9.1			
3	**Southern Hikurangi and Wellington Region faults (A)**	8.5			
4	**Southern Hikurangi and Wellington Region faults (B)**	8.4			
5	**Southern Hikurangi**	8.9			
6	**Western offshore faults (Mascarin)**	7.2			
7	**Fisherman's Fault**	7.2			
8	**Northern Ohariu Fault**	6.9			
9	**Northern Wairarapa Fault**	7.1			
10	**Aotea-Evan's Bay Fault**	6.5			

Figure 3.2 Summary table of location-dependent hazard for all considered scenarios and perils. Warmness of colour is a qualitative assessment of severity. Red is most severe, yellow least.

4.0 REVIEW OF LIFELINES REPORTS

In this section, we review existing lifelines documents to consolidate existing work that provides insights into reliance of each region to critical infrastructure assets and the expected functionality during potential future hazard events. The purpose of this review is to obtain a high-level understanding of the existing knowledge around how each region may perform during future hazard events. It is important to note that this section only reviews pre-existing material and does not consider the potential impacts that may occur from the specific scenarios that have been produced as part of this work.

4.1 Manawatū

4.1.1 Critical Infrastructure Hotspots

An analysis of critical infrastructure hotspots within Manawatū identified the following sites as hotspots (Manawatū-Whanganui Civil Defence and Emergency Management Group 2016; Figure 4.1):

- **Bunnythorpe substation, Palmerston North City:** There is a considerable concentration of electricity assets located at the substation. The report notes that the substation is built to a high seismic standard and is expected to be operational following an earthquake. Transpower have plans in place to provide temporary transmission capacity within a matter of days should the site experience damage.
- **Wharite:** Provides telecommunications, broadcasting and radio services to and throughout the region. Several other lifelines also hold assets at the site. The site was reported to be built to a high seismic standard, but it is located near the Ruahine Fault.
- **East–West Road Connectors**: Routes that connect Palmerston North and Woodville could be affected by earthquakes and severe weather that could result in the closure of these routes.
- **Fitzherbert Bridge, Palmerston North City:** This is a key transportation route, and the bridge contains several critical infrastructure assets.

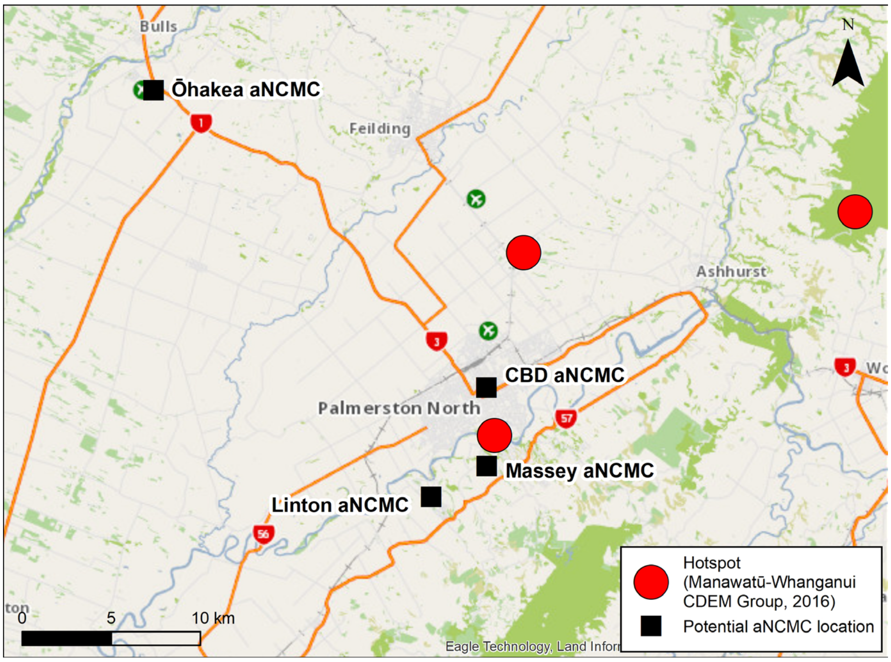

Figure 4.1 Hotspots in Manawatū identified within the 2016 Manawatū-Whanganui Lifelines Report and potential aNCMC locations.

4.1.2 Previously Identified Potential Impacts

The 2016 Manawatū-Whanganui Lifelines Report identified earthquakes, tsunami, volcanic eruption and severe weather as potential hazards that could affect the region. Of these, earthquakes and severe weather are the most likely to have implications for the potential aNCMC locations. The identified tsunami impacts are constrained to Whanganui, Foxton and Koitiata. Volcanic ash could affect Manawatū, but the identified impacts within the region would largely be constrained to removing ash from affected roads (scenarios suggest a few millimetres) or if major electricity infrastructure out of the region was to be affected. Thus, we focus our review on seismic and severe weather in the sub-sections below.

4.1.2.1 Seismic

A national liquefaction susceptibility analysis has found that Palmerston North City is located within a high-liquefaction-susceptibility area (Figure 4.1; Lin 2022). It is important to note that the analysis from Lin (2022) is intended for national-scale analysis and so cannot be used to assess site-specific susceptibility. However, given that much of Palmerston North City is in the high, and in some places very high, susceptibility classes indicates that damage and disruption of services may occur during large earthquakes.

The potential impacts from liquefaction were assessed as part of the 2016 Manawatū-Whanganui Lifelines Report. That analysis used a regional-scale liquefaction susceptibility map that differed from the national-scale assessment of Lin (2022) but provides useful considerations of the potential effects of liquefaction in the region. The report found the following impacts:

- **Wastewater:** Damage or disruption of plants, pumps and pipelines. Bulls was identified in the report as having wastewater assets located within expected liquefaction zones. The Palmerston North wastewater treatment plant and some pump stations are located within high-susceptibility zones, which, if damaged, could lead to partial loss of service for the city.
- **Water supply:** Pipes located in the southern part of Palmerston North were identified as prone to potential damage by future liquefaction, which would disrupt water supply to some parts of the city. Damage to intakes, pumps, pipelines, reservoirs and plants could lead to a loss of supply to Bulls.
- **Electricity:** Distribution in the Palmerston North central business district (CBD) could experience total or partial loss of supply. Several transmission circuits could be affected in Palmerston North.
- **Telecommunications:** Likely to be able to repair any damage before major service disruption occurs.
- **Transportation:** Bulls Bridge was identified as possibly being damaged, requiring repairs in the order of weeks to months, or, potentially, a complete failure.

4.1.2.2 Severe Weather

Sustained or high-intensity rainfall has been identified as the most frequently occurring hazard in the region. Palmerston North City has 1-in-500-year flood-design standards. The 2016 Manawatū-Whanganui Lifelines Report investigated the region's vulnerability to severe weather events using a 1-in-200-year flood model across the region, in addition to hydrological stormwater models for Palmerston North City. Key findings from that analysis were:

- **Wastewater:** Damage or destruction of plants, pumps and pipelines could lead to public health risk or environmental damage. The Bulls wastewater treatment plant was reported as being at recognised risk of damage by flooding. Raw sewage discharge was reported as possible for Palmerston North.
- **Water supply:** Trickers Hill reservoir, which serves Bulls, is located within the 1-in-200-year flood zone used in their analysis. Access to the reservoir was identified as being potentially cut off during such an event. The pipe bridge feeding Trickers Hill reservoir could be destroyed, which would have implications for the water supply in Bulls.
- **Electricity:** Transmission towers are potentially exposed to slips caused by heavy rainfall. Temporary towers could be established within 2–3 weeks and re-building would likely take several months. It is possible that there will be a short-term partial loss of electricity supply to Palmerston North during such events.
- **Telecommunications:** Unlikely to suffer major impacts unless bridges carrying cables are swept away. However, some service disruption could be caused as a result of power outages.
- **Transportation:** The road network could be affected by flooding, scouring, washouts, slips and debris from high winds. All of these effects could cause isolation of some communities and disruption to major transportation routes. Disruption of transportation routes could in turn delay repairs of other affected infrastructure and cause logistics challenges throughout the region (e.g. re-fuelling generators). Bulls Bridge was reported to have a particularly high vulnerability, with potential damage possibly needing weeks to months to repair.

4.2 Auckland

4.2.1 Critical Infrastructure Hotspots

An analysis of Auckland's critical infrastructure hotspots found that the following sites have the highest consequences if all services at that site were to fail (Auckland Engineering Lifelines Group 2017; Figure 4.2).

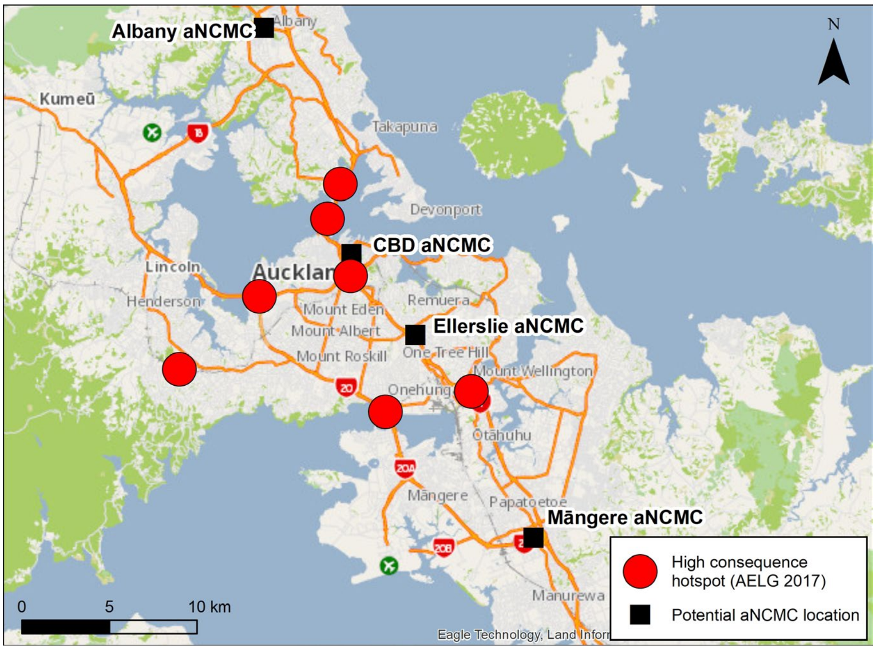

Figure 4.2 Highest consequence hotspots identified in Auckland Engineering Lifelines Group (2017) and potential aNCMC locations.

4.2.2 Previously Identified Potential Impacts

Auckland is exposed to a number of natural hazards, but we focus our review here to the identified potential impacts from tsunami and severe weather, as these are what we anticipate would be the most probable events that could concurrently affect both Wellington and Auckland.

4.2.2.1 Tsunami

The report used a uniform hazard scenario across Auckland, assuming a 3-m-high tsunami, which the report considered as a maximum credible scenario for the region. More in-depth location-specific modelling was then undertaken where it was assumed that the maximum credible scenario would exceed 3 m. Key findings in the report were:

- **Wastewater:** Potentially considerable impacts due to inundation of coastal pump stations and trunk mains crossing bridges. This may require diversion of outflows to safe watercourses, as it is estimated that full reconstruction may take over six months.
- **Water supply:** Local networks in the North Shore and Orewa are likely to be affected. Orewa could lose supply if the trunk supply on the Orewa Estuary Bridge is destroyed.
- **Electricity:** The report finds that the energy sector is unlikely to have major widespread effects, but localised impacts are likely. There are a number of towers and cables that cross low-lying rivers and harbours that could be affected. However, impacts were anticipated to be relatively localised. A number of Vector's substations, cables, poles and pillars were within the modelled inundation zone, and the report estimates that this would have an impact on the supply to approximately 2–4% of the population.
- **Telecommunications:** Some local impacts are anticipated to the cellular and landline network. Cellular is likely to be affected by degradation of capacity as opposed to total loss of coverage. The impacts will be dependent on power failure.
- **Transportation:** Eastern shore roads are highly exposed but often have easily accessible alternative routes. Key coastal infrastructure such as Ports of Auckland, Britomart and ferry terminals may be damaged and could take on the order of months to years to restore.

4.2.2.2 Severe Weather

The major storm event considered within the 2014 AELP report considered a 1-in-100-year tropical cyclone event. The identified impacts for each infrastructure sector were:

- **Wastewater:** Overflows into watercourses and estuarine and marine environments due to system blockages and power failures, leading to potential public health effects if not cleared.
- **Water supply:** Potential for restricted access to dams, pipelines and headworks facilities due to flooding, slips and washouts along roads. High turbidity for an extended period after the storm has passed may lead to restrictions on water-supply use from dams and river-water sources, particularly if the Hunua Ranges are greatly affected. Dams and spillways are capable of coping with a Maximum Credible Event. Multiple metropolitan water treatment plants should ensure that overall supply is maintained. Disruptions are likely to be constrained to localised areas with difficult access.

- **Electricity:** Widespread and short duration electricity interruptions are expected. Some localised areas may have some longer-term (>1 week) outages. There may be localised failure of overhead distribution lines, due to debris from high winds, and poles, due to wind and land instability; and above-ground pillars located within floodplains may be affected by flooding. CBD supply could be disrupted if Vector's Quay substation is heavily flooded (would require >0.3 m inside the substation).
- **Telecommunications:** Minor impacts to the cellular service are expected, but there could be periods of overloading. The landline network could be impacted due to overhead lines being damaged by wind and debris. It is unlikely that broadcasting will be affected. It was anticipated that the cellular network could have full-service restoration in 1–4 days, while the landline network could take 1–10 days.
- **Transportation:** Potential to moderate speeds and close clip on lanes for the Harbour Bridge during high winds are expected, as well as reduced road capacity and speeds, with increased travel times due to localised flooding and debris. Some rail routes may be inaccessible due to debris on the lines. There may be potential impact on marine operations due to storm debris within the shipping channel and berth areas. Auckland Airport runway would be closed during the peak of the storm.

5.0 WORKSHOP OUTCOMES

A workshop was held on 25 August 2022 to discuss the aNCMC business case development and to identify whether the potential scenarios identified capture the necessary range and scope for this project. Subject-matter experts from NEMA, GNS Science, Wellington City Council, Manawatū-Whanganui Council, Toka Tū Ake EQC and Auckland Council participated in the workshop. In this section, we briefly summarise the main outcomes from the workshop process.

5.1 Identifying Potential Regional Vulnerabilities

To identify potential regional vulnerabilities, a brainstorming discussion was facilitated. The intent of this discussion was to identify potential high-level major vulnerabilities to natural hazards that may potentially affect the operation of an aNCMC in each of the regions.

The discussion identified the following potential vulnerabilities:

- Manawatū Region is reliant on fuel delivery from outside the region (trucked in). Thus, there is heavy reliance on road transportation.
- The proximity of Manawatū to Wellington means that, if Wellington is affected by a large earthquake, many impacts will likely be felt in Manawatū as well.
- Staff are a key consideration for site vulnerability:
  - There is possibly a benefit to having an aNCMC reasonably close to Wellington, as the staff that are used to working in an NCMC can do training and potentially access the site. Moving people back and forth from Auckland might be challenging for families.
  - When considering the capability to move staff from Wellington to another region, it may be important to consider where the staff actually live. Staff located on the Kāpiti Coast may be able to access Manawatū quicker than Wellington-based staff due to damaged roads within Wellington.
- Transportation between Manawatū and Wellington may require specific consideration due to the potential requirement to move staff between the regions. Current engineering thinking is that Transmission Gully might be disrupted for about three days before some level of functionality is restored.
- The Fitzherbert Bridge is the only link between the Linton and Massey potential aNCMC locations and Palmerston North, unless a large detour is taken to Ashurst. However, the footbridge at Dittmer Drive has been built to support one New Zealand Defence Force vehicle at a time.

5.2 Brainstorming Natural Hazard Scenarios that Might Affect aNCMC

A brainstorming session was also held to stress-test potential natural hazard scenarios that could concurrently disrupt the NCMC and an aNCMC in Auckland and/or Manawatū. Identified scenarios included:

- Combined impacts from different earthquakes: Alpine Fault, Hikurangi Margin and Wellington Fault. All are expected to have some effect on Manawatū.
- Severe weather and flooding events:
  - It was noted that increasing frequency of severe weather due to climate change may increase the chances of a severe weather event coinciding with a large event, such as an earthquake or tsunami.

- Potential flooding of the Manawatū or Rangitikei rivers.
- A ‘Bola-type’ event could cause widespread disruption in Auckland (e.g. power and access).
- Large subduction zone events and crustal faults can create vertical land displacements that consequently impact flooding hazards.

- The potential for a large subduction-zone earthquake inducing a volcanic eruption was discussed, but the science on this linkage is highly uncertain and unclear.

6.0 POTENTIAL NEXT STEPS

The results presented here represent a preliminary study undertaken within the pre-defined scope of the project. This work has highlighted some challenges with earthquake simulators and the sets of synthetic earthquakes that they generate. Some earthquakes, such as a M_W 8 on the Alpine Fault, which geological evidence strongly supports (Howarth et al. 2021), do not occur in the current version of the simulators. However, this does not mean that an AF8-type event cannot or will not happen. The synthetic earthquakes generated by simulators should be used to expand the range of earthquakes that we consider, not limit them. We specifically suggest a more thorough treatment of Scenario 1 (Alpine Fault and Wairau Fault) and Scenario 2 (full Hikurangi and associated crustal faults). Both events have broad and serious consequences for New Zealand. The occurrence and nature of both events needs to be further examined in the comprehensive New-Zealand-wide synthetic-seismicity context and ground motions from the complex rupture models need to be better quantified. This requires a close examination of the possibility that some of the triggered faults are early aftershocks. While appropriate for its intention of testing factors contributing to the Alpine Fault earthquake cycle, we note that the previous simulator work of Howarth et al. (2021) focused on understanding the role of geometric complexity of the Alpine Fault and was not intended to explore the range of possible fault interactions with other mapped active faults. Subsequent analysis of the risk posed to critical infrastructure from these events also needs to be assessed. In addition, further work is needed to understand the controls on which synthetic earthquakes are generated by earthquake simulators, which we discuss in Appendix 2.

7.0 ACKNOWLEDGEMENTS

This work would not have been possible without significant aligned research under the RNC National Science Challenges Earthquake and Tsunami Programme. The work also utilises modelling frameworks developed under or supported by the EILD and Rapid Characterisation of Earthquakes and Tsunami (RCET) Endeavour programmes.

8.0 REFERENCES

[AELG] Auckland Engineering Lifelines Group. 2014. Auckland Engineering Lifelines Project: Stage 2. Version 1.1. Auckland (NZ): AELG; [accessed 2022 Sep 6]. https://www.alg.org.nz/document-library/critical-infrastructure-reports/

[AELG] Auckland Engineering Lifelines Group. 2017. Auckland Engineering Lifelines Project: Stage 2. Version 2.0. Auckland (NZ): AELG; [accessed 2022 Sep 6]. https://www.alg.org.nz/document-library/critical-infrastructure-reports/

Coffey GL, Langridge RM, Van Dissen RJ, Litchfield NJ, Clark KJ, Morgenstern R, Palmer AS. 2022. Paleoseismology of the northern Ohariu Fault, a study into earthquake recurrence and slip rate. Lower Hutt (NZ): GNS Science. 38 p. (GNS Science report; 2022/52). doi:10.21420/TJK0-MY13.

Clark K, Howarth J, Litchfield N, Cochran U, Turnbull J, Dowling L, Howell A, Berryman K, Wolfe F. 2019. Geological evidence for past large earthquakes and tsunamis along the Hikurangi subduction margin, New Zealand. *Marine Geology*. 412:139–172. doi:10.1016/j.margeo.2019.03.004.

Corominas J, Einstein H, Davis T, Strom A, Zuccaro G, Nadim F, Verdel T. 2015. Glossary of terms on landslide hazard and risk. In: Lollino G, Giordan D, Crosta GB, Corominas J, Azzam R, Wasowski J, Sciarra N, editors. *Engineering Geology for Society and Territory – Volume 2*. Cham (CH): Springer International Publishing. p. 1775–1779.

de Vilder SJ, Massey CI. 2020. Guidelines for natural hazard risk analysis on public conservation lands and waters – Part 2: preliminary hazard and exposure analysis for landslides. Lower Hutt (NZ): GNS Science. 30 p. Consultancy Report 2020/51. Prepared for the Department of Conservation. Revised May 2022.

Dieterich JH, Richards-Dinger KB. 2010. Earthquake recurrence in simulated fault systems. *Pure and Applied Geophysics*. 167(8):1087–1104. doi:10.1007/s00024-010-0094-0.

Dowrick DJ. 2005. Strong ground shaking in the 1855 Wairarapa earthquake. In: Townend J, Langridge RM, Jones A, editors. *The 1855 Wairarapa Earthquake Symposium: 150 years of thinking about magnitude 8+ earthquakes and seismic hazard in New Zealand: proceedings volume*; 2005 Sep 8–10; Wellington, New Zealand. Wellington (NZ): Greater Wellington Regional Council. p. 79–83.

Efron B, Tibshirani RJ. 1994. An introduction to the Bootstrap. New York (NY): Chapman and Hall / CRC. 456 p.

Fry B, Bannister S, Beavan RJ, Bland L, Bradley BA, Cox SC, Cousins WJ, Gale NH, Hancox GT, Holden C, et al. 2010. The M_W 7.6 Dusky Sound earthquake of 2009: preliminary report. *Bulletin of the New Zealand Society for Earthquake Engineering*. 43(1):24–40. doi:10.5459/bnzsee.43.1.24-40.

Gerstenberger MC, Bora SS, Bradley BA, DiCaprio C, Van Dissen RJ, Atkinson GM, Chamberlain C, Christophersen A, Clark KJ, Coffey GL, et al. 2022a. New Zealand National Seismic Hazard Model 2022 revision: model, hazard and process overview. GNS Science. 106 p. (GNS Science report; 2022/57). doi:10.21420/TB83-7X19.

Gerstenberger MC, Van Dissen RJ, Rollins C, DiCaprio C, Chamberlain C, Christophersen A, Coffey GL, Ellis SM, Iturrieta P, Johnson KM, et al. 2022b. The Seismicity Rate Model for the 2022 New Zealand National Seismic Hazard Model. Lower Hutt (NZ): GNS Science. 156 p. (GNS Science report; 2022/47). doi:10.21420/2EXG-NP48.

Gledhill K, Ristau J, Reyners M, Fry B, Holden C. 2011. The Darfield (Canterbury, New Zealand) M_W 7.1 earthquake of September 2010: a preliminary seismological report. *Seismological Research Letters*. 82(3):378–386. doi:10.1785/gssrl.82.3.378.

Grapes RH, Downes G. 1997. The 1855 Wairarapa, New Zealand, earthquake: analysis of historical data. *Bulletin of the New Zealand National Society for Earthquake Engineering*. 30(4):271–368. doi:10.5459/bnzsee.30.4.271-368.

Grapes RH, Holdgate GR. 2014. Earthquake clustering and possible fault interactions across Cook Strait, New Zealand, during the 1848 and 1855 earthquakes. *New Zealand Journal of Geology and Geophysics*. 57(3):312–330. doi:10.1080/00288306.2014.907579.

Gusman AR, Wang X, Power WL, Lukovic B, Mueller C, Burbidge DR. 2019. Tsunami threat level database update. Lower Hutt (NZ): GNS Science. 110 p. (GNS Science report; 2019/67). doi:10.21420/QM31-NA61.

Hamling IJ, Hreinsdóttir S, Clark K, Elliott J, Liang C, Fielding E, Litchfield N, Villamor P, Wallace L, Wright TJ, et al. 2017. Complex multifault rupture during the 2016 M_W 7.8 Kaikōura earthquake, New Zealand. *Science*. 356(6334):eaam7194. doi:10.1126/science.aam7194.

Howarth JD, Barth NC, Fitzsimons SJ, Richards-Dinger K, Clark KJ, Biasi GP, Cochran UA, Langridge RM, Berryman KR, Sutherland R. 2021. Spatiotemporal clustering of great earthquakes on a transform fault controlled by geometry. *Nature Geoscience*. 14(5):314–320. doi:10.1038/s41561-021-00721-4.

Kaiser AE, Balfour NJ, Fry B, Holden C, Litchfield NJ, Gerstenberger MC, D'Anastasio E, Horspool NA, McVerry GH, Ristau J, et al. 2017. The 2016 Kaikōura, New Zealand, earthquake: preliminary seismological report. *Seismological Research Letters*. 88(3):727–739. doi:10.1785/0220170018.

Kaiser A, Holden C, Beavan J, Beetham D, Benites R, Celentano A, Collett D, Cousins J, Cubrinovski M, Dellow G, et al. 2012. The M_W 6.2 Christchurch earthquake of February 2011: preliminary report. *New Zealand Journal of Geology and Geophysics*. 55(1):67–90. doi:10.1080/00288306.2011.641182.

Lane EM, Gillibrand PA, Wang X, Power W. 2013. A probabilistic tsunami hazard study of the Auckland region, part II: inundation modelling and hazard assessment. *Pure and Applied Geophysics*. 170(9–10):1635–1646. doi:10.1007/s00024-012-0538-9.

Langridge RM, Ries WF, Litchfield NJ, Villamor P, Van Dissen RJ, Barrell DJA, Rattenbury MS, Heron DW, Haubrock S, Townsend DB, et al. 2016. The New Zealand Active Faults Database. *New Zealand Journal of Geology and Geophysics*. 59(1):86–96. doi:10.1080/00288306.2015.1112818.

Lin AF. 2022. Seismic exposure and impacts across New Zealand infrastructure networks. Auckland (NZ): University of Auckland. 198 p.

Litchfield NJ, Van Dissen R, Sutherland R, Barnes PM, Cox SC, Norris R, Beavan RJ, Langridge R, Villamor P, Berryman K, et al. 2014. A model of active faulting in New Zealand. *New Zealand Journal of Geology and Geophysics*. 57(1):32–56. doi:10.1080/00288306.2013.854256.

[Manawatū-Whanganui CDEM] Manawatū-Whanganui Civil Defence Emergency Management. 2016. Manawatu-Wanganui Lifelines Group lifelines vulnerability study. Palmerston North (NZ): Manawatū-Whanganui CDEM.

Massey CI, Lukovic B, Huso R, Buxton R, Potter SH. 2021. Earthquake-induced landslide forecast tool for New Zealand: version 2.0. Lower Hutt (NZ): GNS Science. 77 p. (GNS Science report; 2018/08). doi:10.21420/G2TP9V.

Massey CI, Olsen MJ, Wartman A, Senogles A, Lukovic B, Leshchinsky A, Archibald GC, Litchfield NJ, Van Dissen RJ, de Vilder SJ, et al. 2022. Rockfall activity rates before, during and after the 2010/11 Canterbury Earthquake Sequence. *Journal of Geophysical Research Earth Surface*. 127(3):e2021JF006400. doi:10.1029/2021jf006400.

Massey CI, Townsend DB, Jones KE, Lukovic B, Rhoades DA, Morgenstern R, Rosser BJ, Ries W, Howarth JD, Hamling IJ, et al. 2020. Volume characteristics of landslides triggered by the M_W 7.8 2016 Kaikōura Earthquake, New Zealand, derived from digital surface difference modelling. *Journal of Geophysical Research: Earth Surface*. 125(7):e2019JF005163. doi:10.1029/2019jf005163.

Moratalla JM, Goded T, Rhoades DA, Canessa S, Gerstenberger MC. 2021. New ground motion to intensity conversion equations (GMICEs) for New Zealand. *Seismological Research Letters*. 92(1):448–459. doi:10.1785/0220200156.

Pagani M, Monelli D, Weatherill G, Danciu L, Crowley H, Silva V, Henshaw P, Butler L, Nastasi M, Panzeri L, et al. 2014. OpenQuake Engine: an open hazard (and risk) software for the Global Earthquake Model. *Seismological Research Letters*. 85(3):692–702. doi:10.1785/0220130087.

Perrin ND, Heron DW, Kaiser AE, Van Houtte C. 2015. V_S30 and NZS 1170.5 site class maps of New Zealand. In: *New dimensions in earthquake resilience: 2015 New Zealand Society for Earthquake Engineering Technical Conference and AGM*; 2015 Apr 10–12; Rotorua, New Zealand. Wellington (NZ): New Zealand Society for Earthquake Engineering. Paper O-07.

Peng Z, Fry B, Chao K, Yao D, Meng X, Jolly A. 2018. Remote triggering of microearthquakes and tremor in New Zealand following the 2016 M_W 7.8 Kaikōura earthquake. *Bulletin of the Seismological Society of America*. 108(3B):1784–1793. doi:10.1785/0120170327.

Power WL, Burbidge DR, Gusman AR. 2022. The 2021 update to New Zealand's National Tsunami Hazard Model. Lower Hutt (NZ): GNS Science. 63 p. (GNS Science report; 2022/06). doi:10.21420/X2XQ-HT52.

Power WL, Kaneko Y, Becker JS, Lin S-L, Holden C, Mueller C. 2018. Hikurangi response plan: developing a scenario for an Mw 8.9 Hikurangi earthquake, including tsunami modelling and a preliminary description of impacts. Lower Hutt (NZ): GNS Science. 39 p. Consultancy Report 2018/168. Prepared for Hawke's Bay Regional Council.

Richards-Dinger K, Dieterich JH. 2012. RSQSim earthquake simulator. *Seismological Research Letters*. 83(6):983–990. doi:10.1785/0220120105.

Robinson R, Benites RA. 1996. Synthetic seismicity models for the Wellington region, New Zealand: implications for the temporal distribution of large events. *Journal of Geophysical Research: Solid Earth*. 101(B12):27833–27844. doi:10.1029/96jb02533.

Seebeck H, Van Dissen RJ, Litchfield NJ, Barnes PM, Nicol A, Langridge RM, Barrell DJA, Villamor P, Ellis SM, Rattenbury MS, et al. 2022. New Zealand Community Fault Model – version 1.0. Lower Hutt (NZ): GNS Science. 97 p. (GNS Science report; 2021/57). doi:10.21420/GA7S-BS61.

Shaw BE, Fry B, Nicol A, Howell A, Gerstenberger M. 2022. An earthquake simulator for New Zealand. *Bulletin of the Seismological Society of America*. 112(2):763–778. doi:10.1785/0120210087.

Shaw BE, Milner KR, Field EH, Richards-Dinger K, Gilchrist JJ, Dieterich JH, Jordan TH. 2018. A physics-based earthquake simulator replicates seismic hazard statistics across California. *Science Advances*. 4(8):eaau0688. doi:10.1126/sciadv.aau0688.

Stirling M, McVerry G, Gerstenberger M, Litchfield N, Van Dissen R, Berryman K, Barnes P, Wallace L, Villamor P, Langridge R, et al. 2012. National Seismic Hazard Model for New Zealand: 2010 update. *Bulletin of the Seismological Society of America*. 102(4):1514–1542. doi:10.1785/0120110170.

Tullis TE, Richards-Dinger K, Barall M, Dieterich JH, Field EH, Heien EM, Kellogg LH, Pollitz FF, Rundle JB, Sachs MK, et al. 2012. Generic earthquake simulator. *Seismological Research Letters*. 83(6):959–963. doi:10.1785/0220120093.

Wallace LM, Barnes P, Beavan J, Van Dissen R, Litchfield N, Mountjoy J, Langridge R, Lamarche G, Pondard N. 2012. The kinematics of a transition from subduction to strike-slip: an example from the central New Zealand plate boundary. *Journal of Geophysical Research: Solid Earth*. 117(B2):B02405. doi:10.1029/2011jb008640.

Wallace LM, Reyners M, Cochran U, Bannister S, Barnes PM, Berryman K, Downes G, Eberhart-Phillips D, Fagereng A, Ellis S, et al. 2009. Characterizing the seismogenic zone of a major plate boundary subduction thrust: Hikurangi Margin, New Zealand. *Geochemistry, Geophysics, Geosystems*. 10(10):Q10006. doi:10.1029/2009gc002610.

Yao D, Peng Z, Kaneko Y, Fry B, Meng X. 2021. Dynamic triggering of earthquakes in the North Island of New Zealand following the 2016 M_W 7.8 Kaikōura earthquake. *Earth and Planetary Science Letters*. 557:116723. doi:10.1016/j.epsl.2020.116723.

Yin Y, Wiemer S, Kissling E, Lanza F, Rinaldi AP, Gerstenberger M, Fry B. 2021. Seismicity rate change as a tool to investigate delayed and remote triggering of the 2010–2011 Canterbury Earthquake Sequence, New Zealand. *Bulletin of the Seismological Society of America*. 111(4):2248–2269. doi:10.1785/0120210006.

APPENDICES

This page left intentionally blank.

APPENDIX 1 PHYSICS-BASED EARTHQUAKE SIMULATORS

A1.1 RSQsim

The scenarios outlined in this report were generated using the RSQsim earthquake simulator (Dieterich and Richards-Dinger 2010; Richards-Dinger and Dieterich 2012). Earthquake simulators are “computer programs that use the physics of stress transfer and frictional resistance to describe earthquake sequences” (Tullis et al. 2012). Such programs offer the possibility of providing catalogues of potential earthquakes over much longer timescales than instrumental, historical or paleoseismological records and have been shown to produce a good statistical fit to observed seismicity both in Aotearoa New Zealand (Shaw et al. 2022) and in California (Shaw et al. 2018). Simulators differ in the physics that they incorporate (for example, some model the crust as purely elastic, whereas others incorporate viscoelastic effects) and the ways in which they ‘describe’ earthquake sequences, whether that be purely statistical, a series of earthquakes on a single fault or synthetic slip distributions on multiple faults over hundreds of thousands of years.

Common to earthquake simulators such as RSQsim, which are designed to generate catalogues of synthetic earthquake slip distributions, is their use of a deformation model consisting of a 3D fault network and the associated slip rates on these faults. Most of the scenarios we describe here are from the synthetic earthquake catalogue for Aotearoa New Zealand developed by Shaw et al. (2022), which uses an adapted version of the Stirling et al. (2012) fault model as the fault network. Although, in theory, this fault network has been adapted to ensure that there are no geophysically implausible intersections of faults at depth (Shaw et al. 2022), the development of scenarios for this report has demonstrated multiple instances of such intersections and that they may provide a barrier to rupture propagation, as discussed for individual scenarios below. This fault model also uses a highly simplified geometry for the Hikurangi subduction zone (three planar sections). Incorporating an updated geometry for this interface and the full network of faults in the recently published New Zealand Community Fault Model (Seebeck et al. 2022), without intersections at depth, is an ongoing subject of research. The deformation model for this synthetic catalogue uses fault slip rates from Litchfield et al. (2014) to derive fault stressing rates. These rates are then modified following the hybrid loading approach described by Shaw et al. (2018); in effect, the stressing rates are tapered at the edges of the fault surfaces to prevent stress discontinuities.

A key differentiating feature of RSQsim compared to other earthquake simulators is the use of rate-and-state friction to describe the frictional state of faults and to determine when and where synthetic earthquakes occur. At each timestep, the driving stress on each element is compared to the steady-state shear stress (the shear stress at constant normal stress and slip speed), with three potential states: (1) healing, where the driving stress is less than the steady state stress and no stress is transferred to adjacent elements; (2) nucleation, when driving stress is greater than the steady state stress, leading to decreasing fault strength and increasing slip speed on slip-weakening patches; and (3) rupture, when the slip speed reaches a defined seismic slip speed. The first two states are quasi-static, but the third is quasi-dynamic and assumes a constant slip speed, updating the system at each timestep with the stress changes applied to other fault patches by those which are rupturing (Richards-Dinger and Dieterich 2012). As such, RSQsim represents an approximation to rate-and-state friction, which does not include the full effects of rupture dynamics, including seismic wave propagation. Further testing is required to explore the key parameters to which the synthetic earthquake catalogues are sensitive and the consistency of the generated slip distributions with observations. This testing is ongoing as part of the Resilience to Nature’s Challenges 2 project. We present a comparison of a 5000- and 500-year window of the catalogue to the catalogue of historic seismicity (1940–2010) to highlight the variation in the synthetic catalogue over different timescales in Figure A1.1. We show catalogue recurrence by magnitude in Figure A1.2.

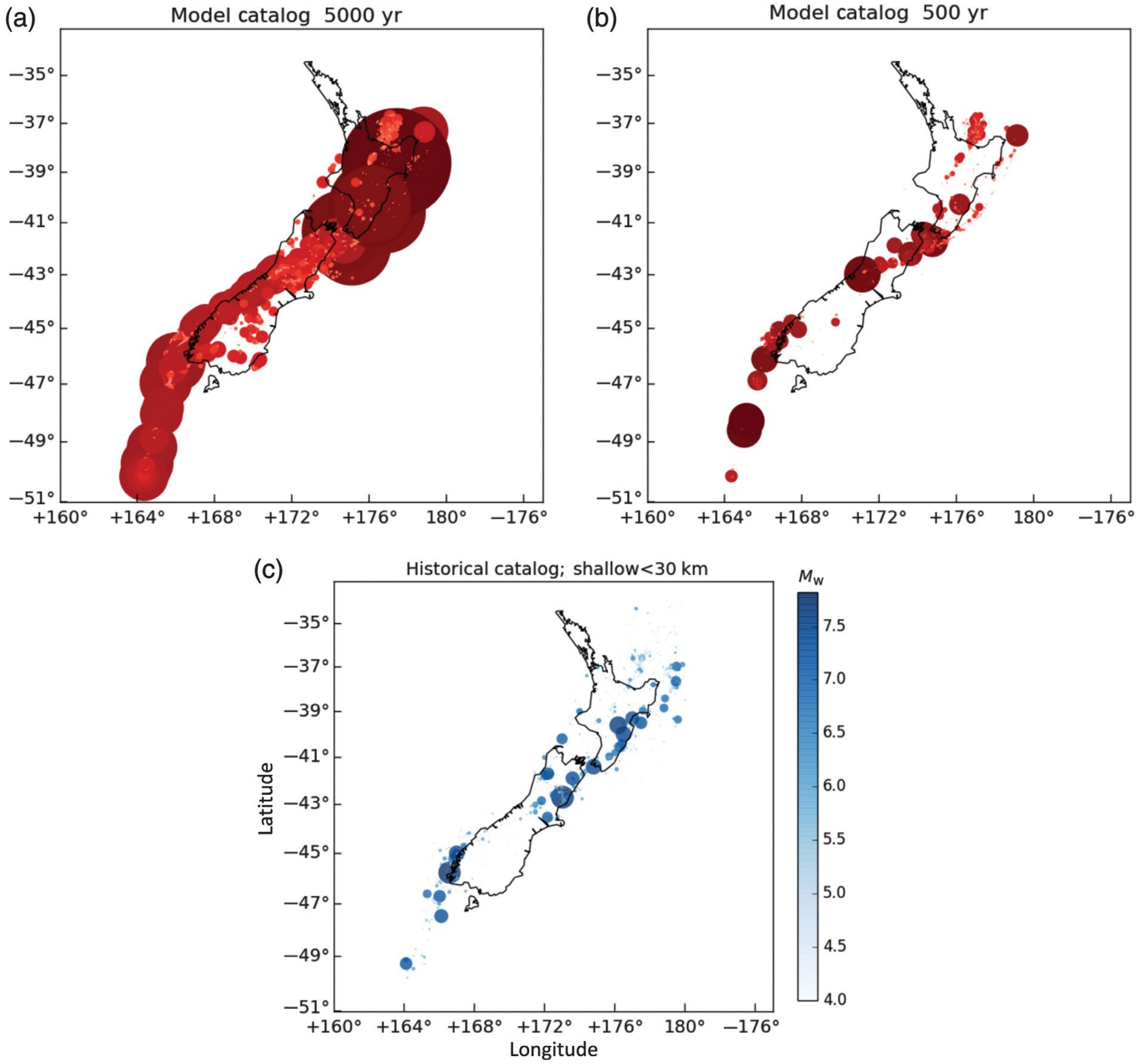

Figure A1.1 Synthetic long-term (A), synthetic short-term (B) and historical earthquake epicentre catalogues presented in Shaw et al. (2022). The historic catalogue has many fewer M_W 7.5+ earthquakes, presumably due to its relatively short duration.

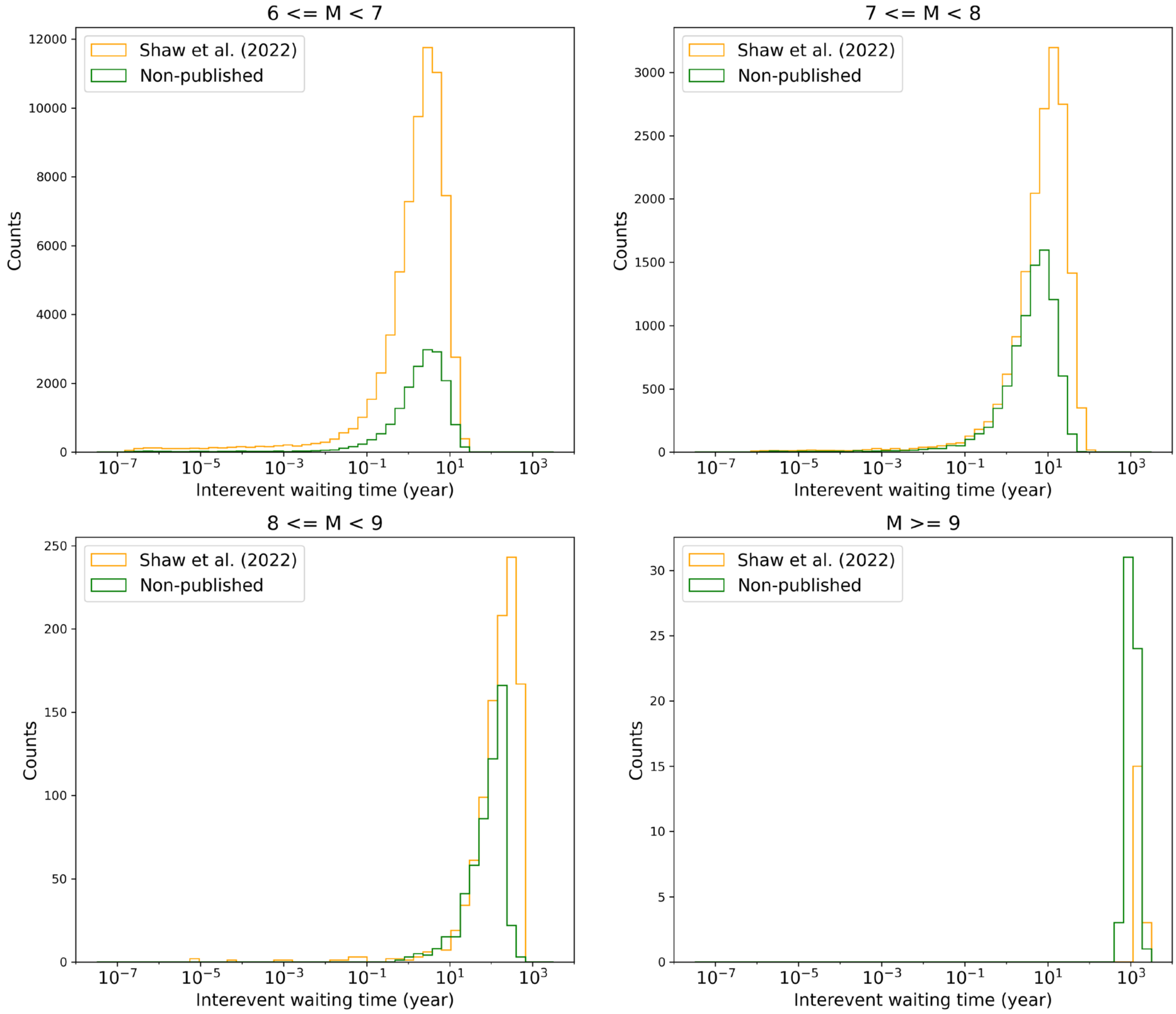

Figure A1.2 Inter-event plots for M6–M7, M7–M8, M8–9 and M9+. The magnitude ranges represent earthquakes in the entire model and do not show recurrence on a specific fault (i.e. Alpine Fault or Hikurangi megathrust), although the biggest events only occur in conjunction with the Hikurangi megathrust.

APPENDIX 2 SCENARIOS

We have extracted scenarios from the synthetic seismicity catalogue with particular characteristics relevant to Wellington hazard, notably strong shaking, because of their proximity to the capital. These scenarios are intended to represent suites of events that occur in the catalogue. Below, we discuss 10 of these scenarios, their relevance to combined seismic hazard in Wellington and Palmerston North and some of the associated caveats.

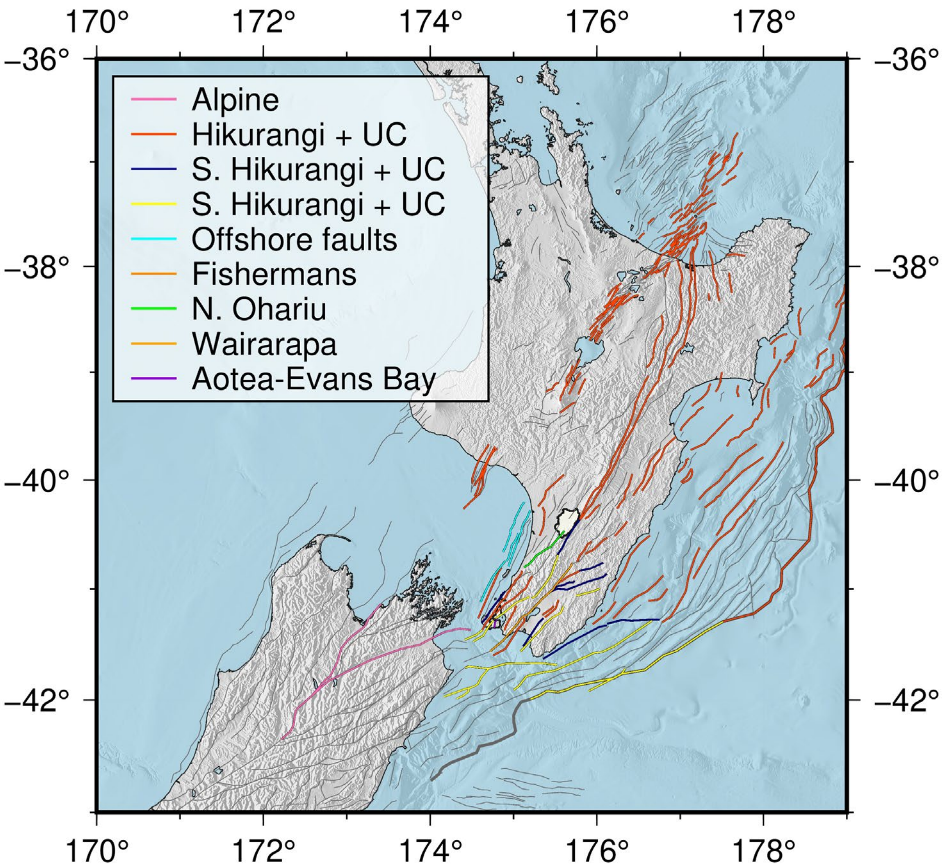

Figure A2.1 Map of faults involved in different rupture scenarios. Grey lines are faults in the New Zealand Community Fault Model (Seebeck et al. 2022) that are not involved in any of the scenarios. The colours correspond to faults moving in different scenarios outlined in this appendix. Note that some faults rupture in more than one scenario.

A2.1 Scenario 1: Alpine Fault and Wairau

Strong ground motions in Wellington resulting from the 2016 Kaikōura earthquake highlighted the importance of considering South Island earthquakes in understanding seismic hazard in Wellington. At the same time, AF8, an emergency-planning scenario developed around the possibility of a M_W 8 earthquake occurring on the Alpine Fault (https://af8.org.nz/), has drawn attention to the Alpine Fault as a major source of seismic hazard. We therefore looked for synthetic earthquakes in the catalogue that involved both the Alpine Fault and faults further to the north, such as the Waimea and Wairau faults. Initially, we searched for synthetic earthquakes involving both the Alpine Fault and southern segments of the Wellington Fault, However, there are no events in the current version of the synthetic earthquake catalogue that involve both the Alpine and Wellington Hutt Valley faults. This lack of events is probably because of the lack of fault connectivity across the Cook Strait in the current fault model (Grapes and Holdgate 2014).

Additionally, Mw 8 events on the Alpine Fault in the synthetic catalogue all involve more southerly sections of the fault (the Jacksons–Kaniere section) and do not propagate further north. Synthetic earthquakes that rupture both the Alpine Fault and faults to the north all have M_W <8. The absence of particular earthquakes in the synthetic earthquake catalogue does not mean that such earthquakes cannot occur, or that they should not be planned for, but probably reflect the sensitivity of the simulator results to fault geometry or loading rates, which are the subject of ongoing research. The scenario shown in Figure A2.2 is a M_W 7.7 synthetic earthquake, involving the Wairau, Alpine and Waimea faults. The earthquake starts at the junction between the Waimea South (Flaxmore-Waimea-Tahunanui in the New Zealand Community Fault Model [NZCFM; Seebeck et al. 2022]), Wairau and Alpine faults. Slip propagates southwards on the Alpine Fault for about 35 s before a northwards rupture starts on the Wairau Fault. Both the Alpine and Wairau faults slip by up to 6 m. In total, 57% of the energy release in the synthetic earthquake occurs on the Wairau Fault, 42% on the Alpine Fault and the remaining 1% on the Waimea South Fault.

RSQsim (the physics-based simulator we use here) captures some, but not all of, the full physics of how earthquake ruptures evolve through time. However, the propagation of slip in this event in both directions away from the hypocentre (i.e. ‘bilateral rupture’) is an important consideration for hazard, as rupture directivity promotes an asymmetric distribution of ground motion amplification. Directivity amplification can increase the severity of ground shaking, especially at long periods that commonly affect larger infrastructure. The position of Wellington along strike from the Wairau Fault means that a northeastwards rupture on this fault would be likely to lead to high ground accelerations in Wellington and Nelson.

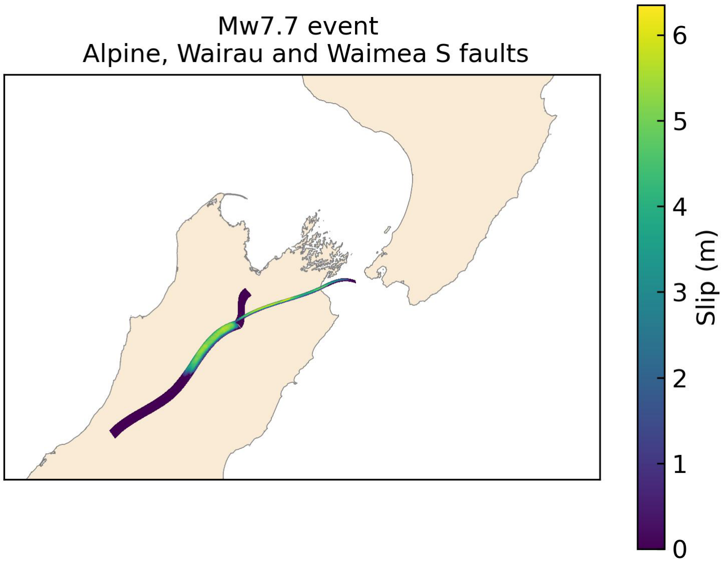

Figure A2.2 Event 1844079.

A2.2 Scenario 2: Full Hikurangi and Upper Crustal Faults

Wellington lies directly above the Hikurangi subduction zone, which is thought to be capable of producing M_W 9 earthquakes (e.g. Wallace et al. 2009). The Hikurangi Response Plan, based on an earthquake scenario developed by GNS Science (Power et al. 2018), looks in detail at the likely impacts of a large earthquake on the subduction interface and the associated tsunami. The main scenario described in that report has the highest slip beneath the Wairarapa Fault, near Wellington. However, what that scenario does not include is the possibility of upper-crustal faults triggering or being triggered by movement on the subduction interface. It is (and is likely to remain) unclear to what extent the Hikurangi subduction interface was involved in the 2016

Kaikōura earthquake (Hamling et al. 2017), but that earthquake demonstrated the importance of considering multi-fault ruptures in seismic hazard. There is also ongoing debate about the extent to which vertical motions along the coast of the North Island are related to slip on the subduction interface, as opposed to the movement of shallower crustal faults, but the possibility of simultaneous, or near-simultaneous, rupture on such faults cannot be ruled out. Clark et al. (2019) discuss how it is difficult to differentiate upper-plate fault deformation from subduction interface deformation. In the synthetic earthquake catalogue used here, we typically see crustal faults activated during large (M8+) subduction zone events. Again, we highlight challenges in interpreting secondary fault activation as coseismic triggering or early aftershocks. We suggest that the scenario be considered a possible sequence that could or could not happen within the first minutes of the main shock.

The second reason for including this scenario is to look at the effects of crustal faults in the Wellington region (such as the Wellington Hutt Valley and Wairarapa faults) rupturing in the same event as faults near Manawatū (such as the Mohaka and Wellington Pahiatua faults). The synthetic earthquake catalogue does not contain any events that rupture both of these sets of faults without the subduction interface also moving. The absence of such events in the synthetic catalogue does not mean that they cannot occur. It is more likely that the specific intersections of fault used in the model controls which synthetic events are generated.

The scenario shown in Figure A2.3 is a synthetic earthquake that ruptures all segments of the Hikurangi subduction zone *and* multiple crustal faults over a wide region of the North Island. Such an event would have the potential to impact both Wellington and Manawatū, as well as major cities such as Napier and Gisborne. This synthetic earthquake has a moment magnitude of 9.1. The event nucleates on the central Hikurangi and ruptures bilaterally along the subduction interface, with about 25 m of slip along much of the Hikurangi subduction interface. Upper-crustal faults throughout the North Island experience up to about 8 m of slip. Eleven of these faults move in events with an equivalent moment magnitude of 7 or greater. Nearest Wellington, these faults include the Wellington Hutt Valley and Wairarapa faults. Near Palmerston North, they include the Mohaka South fault, the Alfredton North – Makuri-Waewaepa faults and the Mascarin fault (which is discussed in more detail below).

There are several caveats associated with this event, which we believe can be viewed as a maximum credible scenario. First, if an earthquake of this type were to occur, it would be unlikely to take the exact form that we see in this synthetic event. Although this type of event (full Hikurangi rupture with upper-crustal faults in an M_W >9 event) occurs several times over the ~300,000-year duration of the synthetic catalogue, these events are relatively rare and involve slightly different combinations of slip on different faults. Second, the geometry of the subduction interface used in this model is very simplified compared to our current understanding. The model also does not account for coupling variations along the interface (e.g. Wallace et al. [2012], although the effect of such variations on the seismogenic potential of the interface is subject to ongoing debate). Both of these factors might reduce the probability of such uniform high slip across the subduction interface. Third, as essentially all of the upper-crustal faults in the model rupture in this event, it is important to consider whether there might be faults missing and also how these upper-crustal faults interact. This version of the synthetic earthquake catalogue uses the Stirling et al. (2012) fault model that allows faults to intersect at depth, which may not be geologically sensible.

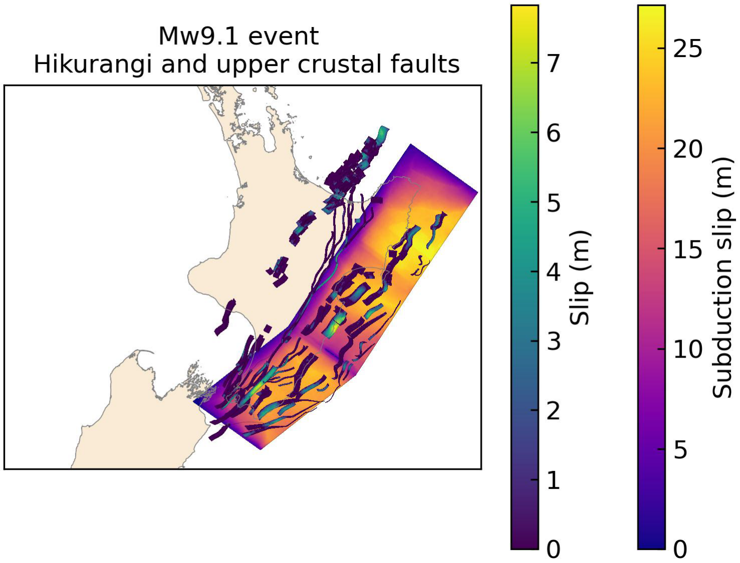

Figure A2.3 Slip distribution for event 759464. Slip on crustal faults and the subduction interface are shown with separate colour bars.

A2.3 Scenarios 3 and 4: Southern Hikurangi and Wellington Region Faults

As well as events that rupture the whole subduction interface and crustal faults throughout the North Island, the synthetic catalogue also includes events that involve only the southern part of the subduction interface but also trigger upper-crustal faults in both Wellington and Manawatū. Here, we show two such synthetic events.

The first of these events is discussed in detail by Shaw et al. (2022). It is a M_W 8.4 event involving faults from the northern South Island to north of Wellington. Most of the energy release on upper-crustal faults in this event occurs on the Wellington Hutt Valley and Wairarapa faults, but there is also slip on the Northern Ohariu Fault closer to Manawatū. Recent work has shown that, in the four most recent events, failure of the Ohariu Fault does not coincide with events on the Hikurangi megathrust fault (Coffey et al. 2022). This highlights the fact that the earthquake simulator is not an earthquake predictor. Scenarios should be used to understand the larger physical phenomena that drives earthquake dynamics and fault interaction. The directionality of the event, which propagates from south to north on the subduction interface, might also increase ground accelerations in the Manawatū region, an effect not captured in the simple ground-motion simulations we use here.

The second of these events is a M_W 8.5 earthquake that again ruptures the southern Hikurangi interface from south to north. In this event, slip propagates further northwest on the Wairarapa fault. There is also more slip on faults towards Manawatū in this event, such as the Wellington Tararua and Pahiatua faults.

These two synthetic earthquakes demonstrate the variability of similar events in the catalogue, and the multiple potential combinations of upper-crustal faults that could rupture together and impact both Wellington and Manawatū. Both events also show the limitations of the current model set-up, where earthquakes tend to start along the edges of fault planes (in this case, the southwestern margin of the Hikurangi), which likely reflects stress concentrations in the model that may not exist geologically.

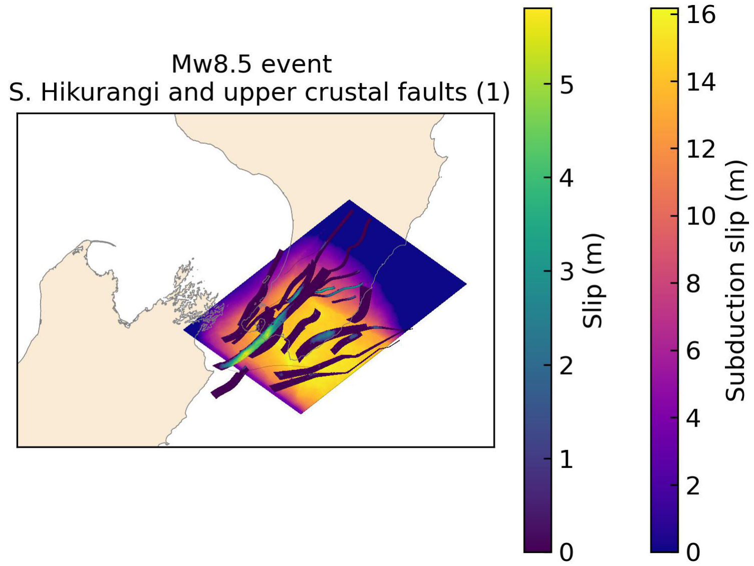

Figure A2.4 Slip distribution for event 292713. Different colour bars are used for slip on the subduction interface and upper-crustal faults.

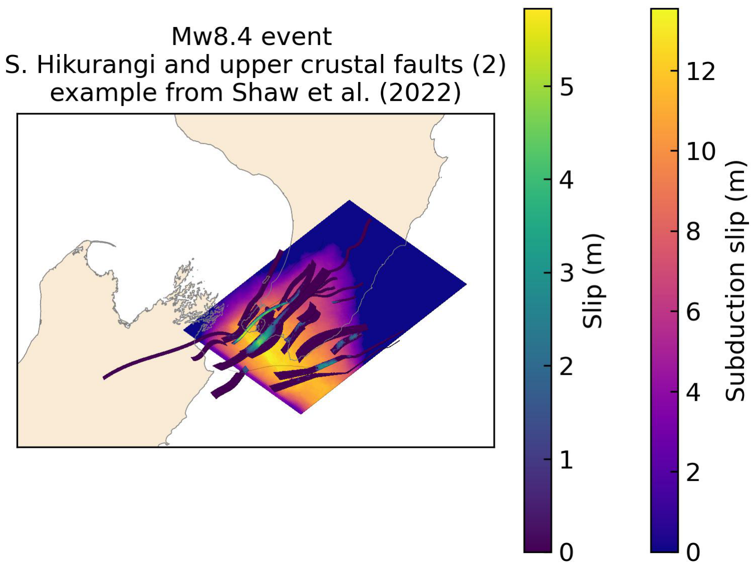

Figure A2.5 Slip distribution for event 1002623, discussed in detail in Shaw et al. (2022). Slip on upper-crustal faults and the subduction interface is shown using different colour palettes.

A2.4 Scenario 5: Southern Hikurangi

Not all earthquakes on the subduction interface will necessarily rupture either the full length of the Hikurangi or both the subduction interface and upper-plate faults. The synthetic earthquake shown in Figure A2.6 is an example of an event that ruptures just the southern section of the Hikurangi, but where high ground accelerations would nonetheless affect both Wellington and Manawatū. This event is from a different catalogue than the others shown in this report, which only simulates events on the subduction interface. As a result, these simulations can include a more realistic geometry for the subduction interface and are able to incorporate along-strike variations in coupling. Including this more complex geometry for the subduction interface in models that also contain upper-crustal faults is a key area of future work.

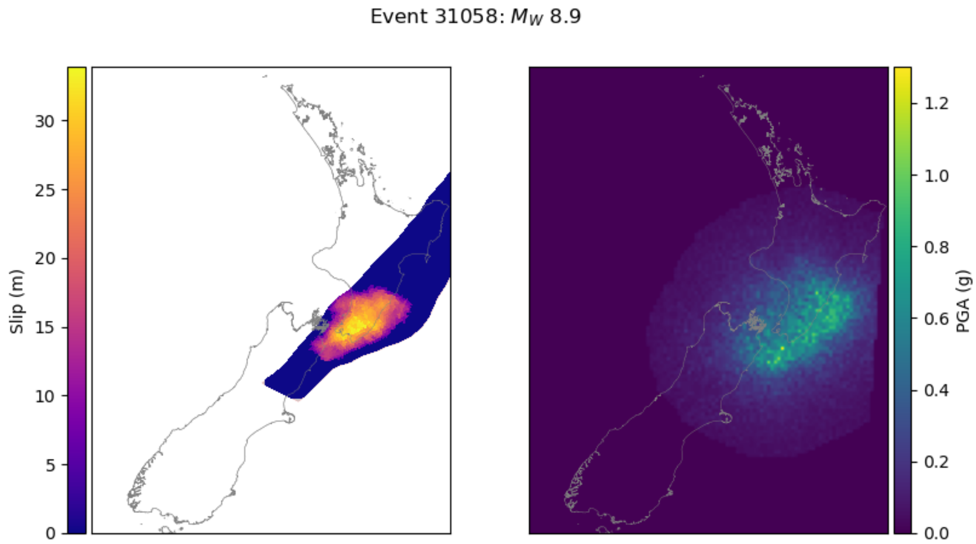

Figure A2.6 Slip distribution and associated peak ground accelerations for a southern Hikurangi earthquake.

A2.5 Scenario 6: Multi-Fault Rupture of Western Offshore Faults (Mascarin)

The following three scenarios consider upper-crustal faults and fault networks that could potentially affect both Wellington and Manawatū in a single event. Although there are several combinations of faults that could intuitively rupture in a multi-fault event (such as the Ohariu faults or the different sections of the Wellington Fault), many of these combinations do not occur in the synthetic catalogue. This does not mean that these faults are not able to rupture together, but we focus here on some combinations that we do see in the synthetic catalogue.

The faults offshore northwest of the Kāpiti Coast are one such group of faults. There are about 20 events in the synthetic earthquake catalogue that rupture some combination of these faults in a magnitude 7 or greater earthquake. Most of these are dominated by slip on the Mascarin Fault, about 17 km offshore, to the west of Palmerston North. These events also include slip on faults further towards Wellington, such as the Fisherman's Fault. The event shown in Figure A2.7 is an example of this kind of earthquake. This example is a M_W 7.2 event that ruptures the Mascarin Fault bilaterally, meaning that slip in a similar earthquake would be directed towards both Wellington and Manawatū. As noted above, the directivity of events only gives a sense of what is possible rather than what would actually happen in a similar earthquake.

The updated fault network in the NZCFM contains additional faults, such as the Otaheke Fault, that are not in the version of the simulation we have used here. Including these additional faults is likely to mean that we see a wider variety of offshore earthquakes in future versions of the simulations and may affect which faults rupture together.

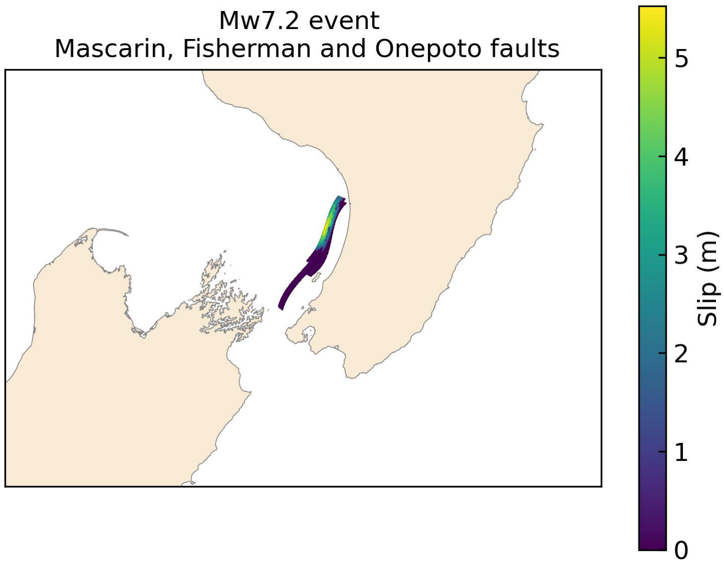

Figure A2.7 Slip distribution for event 950175, involving the Mascarin, Onepoto and Fisherman faults.

A2.6 Scenario 7: Fisherman's Fault

The Fisherman's Fault runs approximately southwest to northeast offshore of the Kāpiti coast. As such, it is one of the faults where an earthquake could affect both Wellington and Manawatū. Figure A2.8 shows an example of a synthetic M_W 7.2 earthquake on this fault. There are 11 similar synthetic earthquakes in the catalogue. None of these synthetic earthquakes rupture the full extent of Fisherman's Fault, probably because the current fault model has the Fisherman's and Mascarin faults intersecting at the approximate northwards limit of slip in this event. Fault intersections provide a barrier to earthquake slip. In a future version of the simulation, we would use a geometry more consistent with geological understanding, where these faults do not intersect at depth, which might lead to larger synthetic earthquakes on this fault.

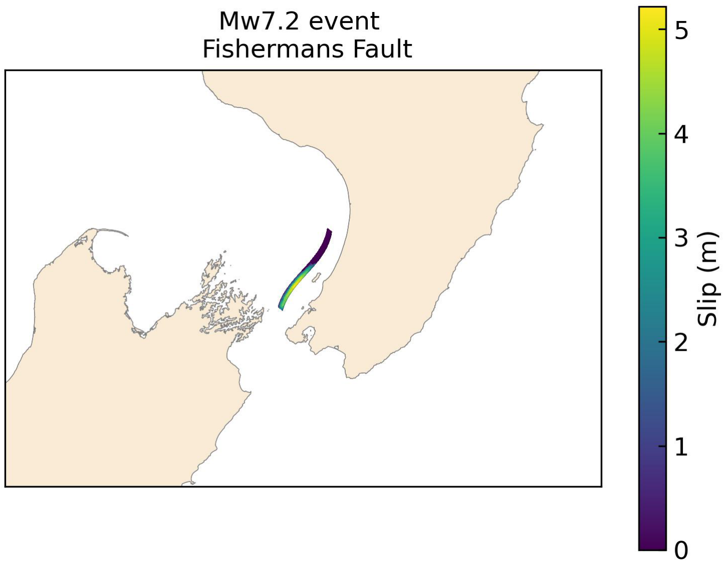

Figure A2.8 Slip distribution for event 1010458 on the Fisherman's fault.

A2.7 Scenario 8: Northern Ohariu

The Northern Ohariu Fault is located southwest of Palmerston North, along strike from the Ohariu Fault, which runs through Porirua, west of Wellington. There are no events in the synthetic catalogue that rupture both of these faults without involving the subduction interface (as in Scenarios 2 and 3 above). Paleoseismic studies have shown that the last two earthquakes on the Northern Ohariu fault coincide with earthquakes on Ohariu fault but not on the subduction zone (Coffey et al. 2022). However, a M_W 6.9 on the Northern Ohariu fault, as shown in Figure A2.9, could potentially impact both Wellington and Manawatū. This scenario gives a sense of the potential impacts of a moderate magnitude earthquake occurring on one of the low-slip-rate faults between Wellington and Manawatū.

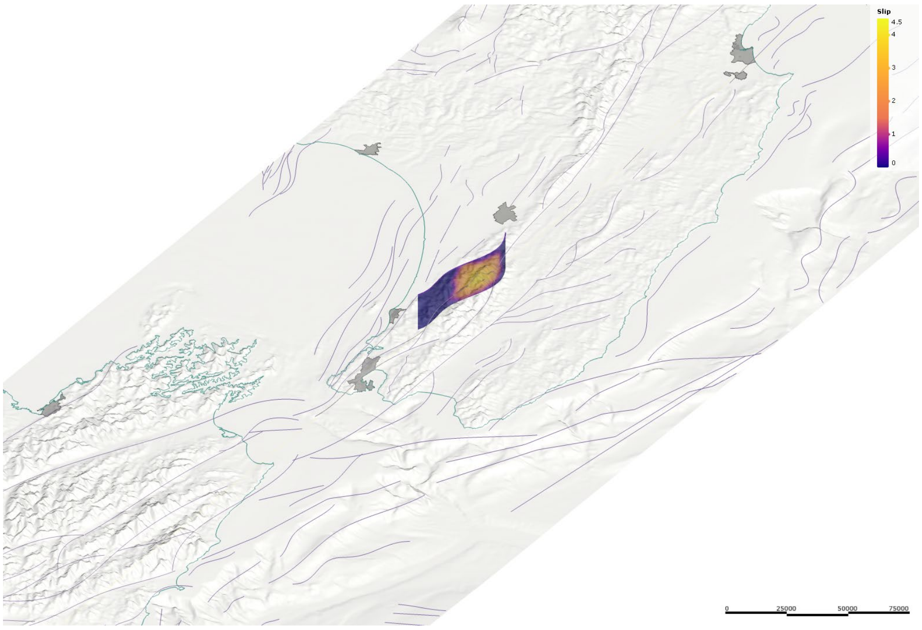

Figure A2.9 Slip distribution for event 1237478 on the Northern Ohariu fault.

A2.8 Scenario 9: Northern Wairarapa

The Wairarapa Fault, east of Wellington, is a major fault thought to have been the source of the 1855 earthquake that caused major damage in Wellington and severe shaking over a wide region (including estimated intensities of 8 in what is now Palmerston North; Grapes and Downes 1997). The potential impacts on Wellington of an earthquake on this fault were discussed extensively in a targeted symposium in 2005 (Dowrick 2005). In the synthetic catalogue, the largest events involving the Wairarapa Fault but not the subduction interface include slip on the Wharekauhau Fault and sometimes the Jordan-Kekerengu-Needles Fault to the south. However, these scenarios require further investigation because, in the current model, the Wharekauhau Fault intersects the Wairarapa Fault at depth, which is not consistent with the most likely geological structure. Probably as a result of this intersection, there are no events in the synthetic catalogue that rupture the whole length of the Wairarapa Fault. The event shown in Figure A2.10 is an example of a M_W 7.4 earthquake rupturing the northern half of the Wairarapa Fault. Such an event would be likely to cause significant ground shaking in both Wellington and Manawatū.

As for several of the other scenarios discussed above, the fault geometry used as an input to the earthquake simulator needs to be refined in order to more fully investigate the range of potential scenarios involving the Wairarapa Fault, particularly potential multi-fault earthquakes involving both this fault and faults further north or west.

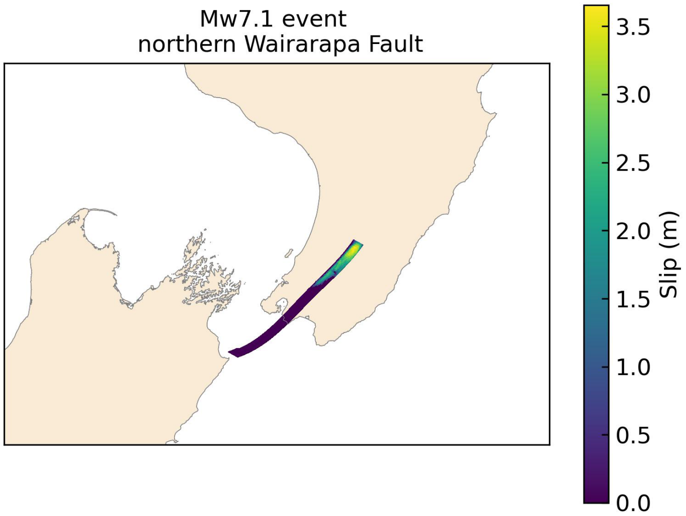

Figure A2.10 Slip distribution for event 19118 on the northern part of the Wairarapa fault.

A2.9 Scenario 10: Local Wellington Earthquake: Aotea – Evans Bay Fault

The Christchurch earthquake of 22 February 22 2011 highlighted the potential for a relatively small-magnitude earthquake located directly beneath a city to have major, long-lasting impacts. The Aotea – Evans Bay Fault runs directly below central Wellington. The scenario shown in Figure A2.11 is a M_W 6.5 synthetic earthquake on this fault. Although the shaking from such an event is unlikely to be significant as far away as Manawatū, the shaking would likely be sufficient to cause significant infrastructural damage around the Wellington region and is therefore included for planning purposes. The Aotea – Evans Bay Fault is not included in the version of the synthetic earthquake catalogue that we used to generate the rest of the scenarios described above. We have therefore used an event from a subsequent version of the catalogue. However, there are, issues with the fault geometries in this catalogue that require further work. There are events in this synthetic catalogue that rupture both the Aotea – Evans Bay and the Wairarapa/Wellington faults further north (without involving the subduction interface), but further work is required to investigate whether these are robust features of the catalogue.

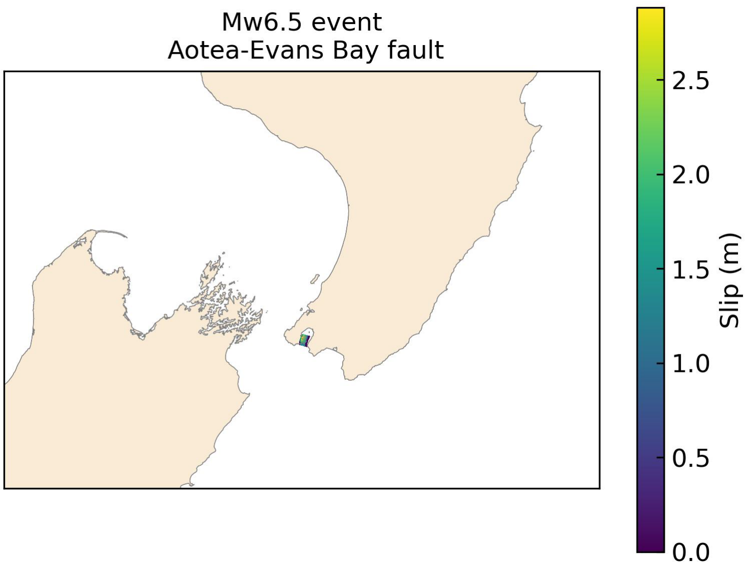

Figure A2.11 Slip distribution for a synthetic earthquake on the Aotea – Evans Bay fault.

APPENDIX 3 RECURRENCE INTERVALS OF LARGE MAGNITUDE EVENTS WITH CRITERIA INCLUSIVE OF THE ANCMC SCENARIOS, AS REPRESENTED BY THE NEW ZEALAND NATIONAL SEISMIC HAZARD MODEL 2022

Table A3.1 lists the recurrence intervals for events of equal or greater magnitude for regions surrounding the scenarios presented in this report, as represented in the source models implemented by the New Zealand National Seismic Hazard Model 2022 (Gerstenberger et al. 2022b). These recurrence intervals are based on participation rates. Participation rates are derived by counting the ruptures or fractions thereof within a given regional polygon, irrespective of their nucleation (or hypocentre) locations. The source models are: (1) crustal-fault-based inversions of geologic and geodetic slip rates with either time-independent or -dependent constraints and applied regional seismicity parameters; (2) inversion of geodetic slip rates on the subduction interfaces; and (3) distributed seismicity models, including the slab source model. Figures A3.1–A3.10 show the respective analyses.

Table A3.1 Recurrence intervals of large magnitude/scenario events for the selected regions, as given by the source models of the New Zealand National Seismic Hazard Model 2022, are summarised in terms of median and range (minimum and maximum in brackets) for the specified magnitude range.

Code	Region	Magnitude Range	Recurrence Interval (Years)
Scenario 1	South Island	$M_W \geq 7.7$	67 (31, 180)
Scenario 2	North Island	$M_W \geq 9.1$	4934 (1312, 21589)
Scenario 3	Southern North Island	$M_W \geq 8.5$	835 (219, 5344)
Scenario 4	Southern North Island	$M_W \geq 8.4$	659 (184, 5344)
Scenario 5	North Island	$M_W \geq 8.8$	2605 (608, 21589)
Scenario 6	Offshore Southern North Island	$M_W \geq 7.2$	345 (126, 855)
Scenario 7	Offshore Southern North Island	$M_W \geq 7.2$	345 (126, 855)
Scenario 8	Wellington	$M_W \geq 6.9$	278 (90, 924)
Scenario 9	Wairarapa	$M_W \geq 7.1$	100 (36, 282)
Scenario 10	Wellington	$M_W \geq 6.5$	235 (81, 603)

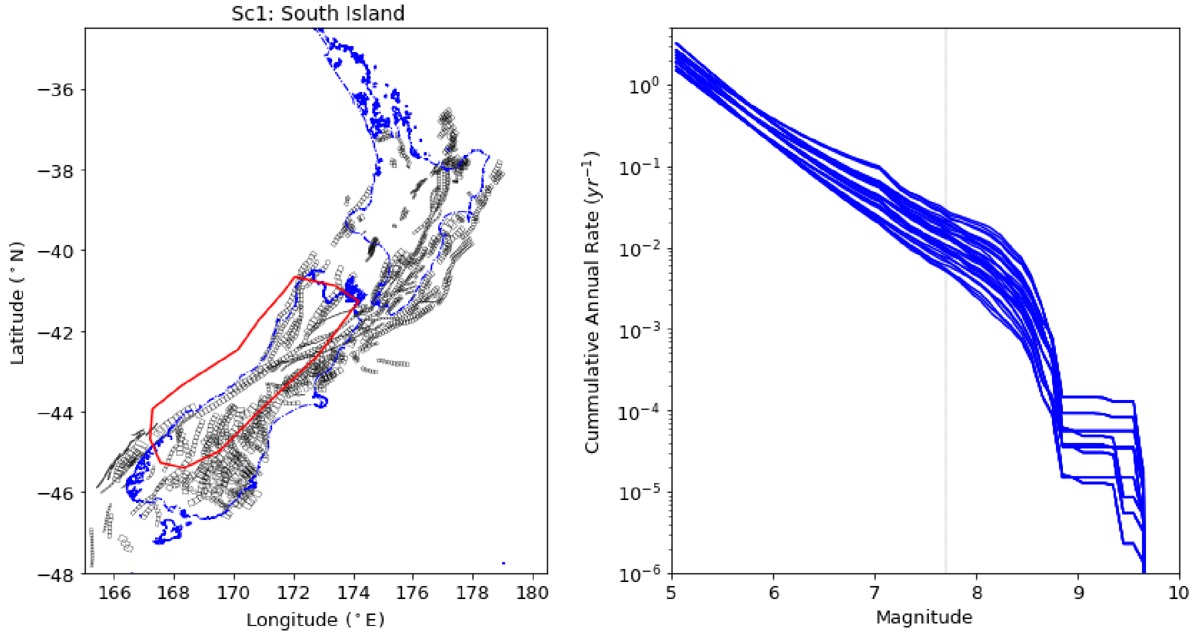

Figure A3.1 Scenario 1: Right: the map depicts the applied spatial polygon (in red) for the analysis of the fault zone (as indicated on the plot) and also the community fault model (black boxes). Left: the magnitude frequency distributions given by the New Zealand National Seismic Hazard Model 2022. The thin line indicates the minimum magnitude of interest.

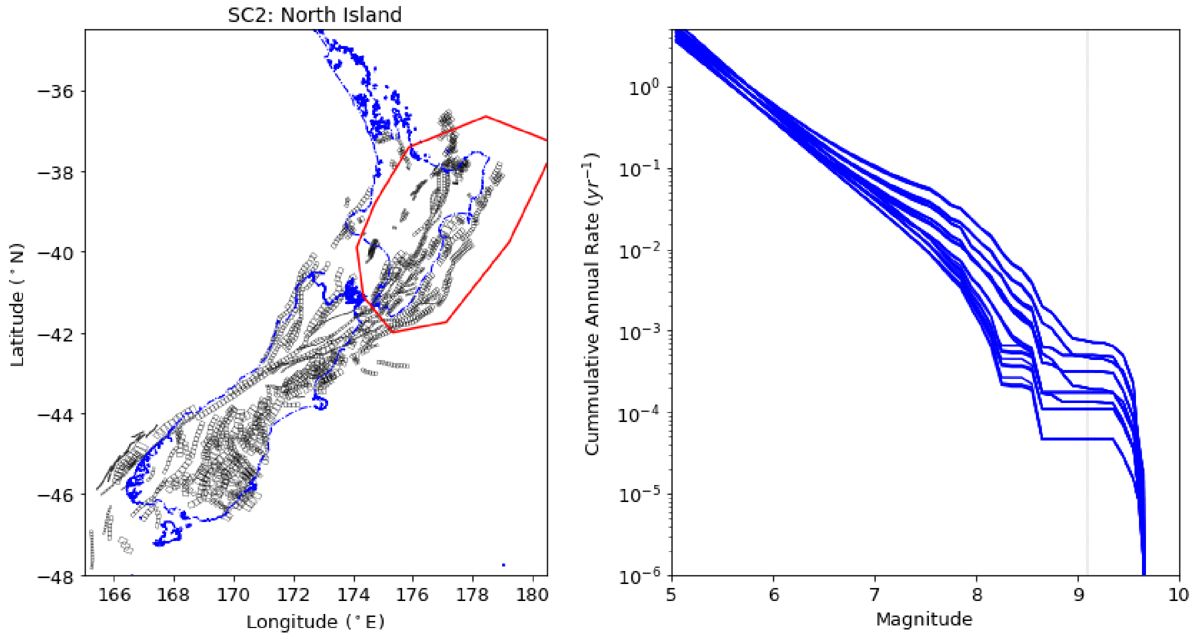

Figure A3.2 Scenario 2: As in Figure A3.1.

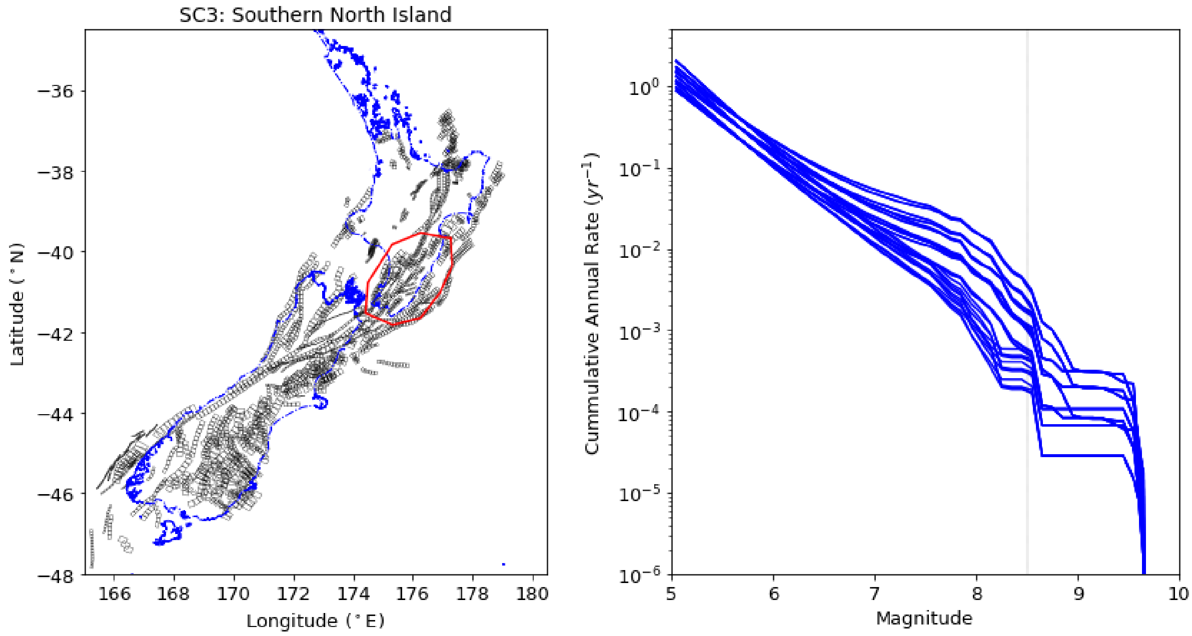

Figure A3.3 Scenario 3: As in Figure A3.1.

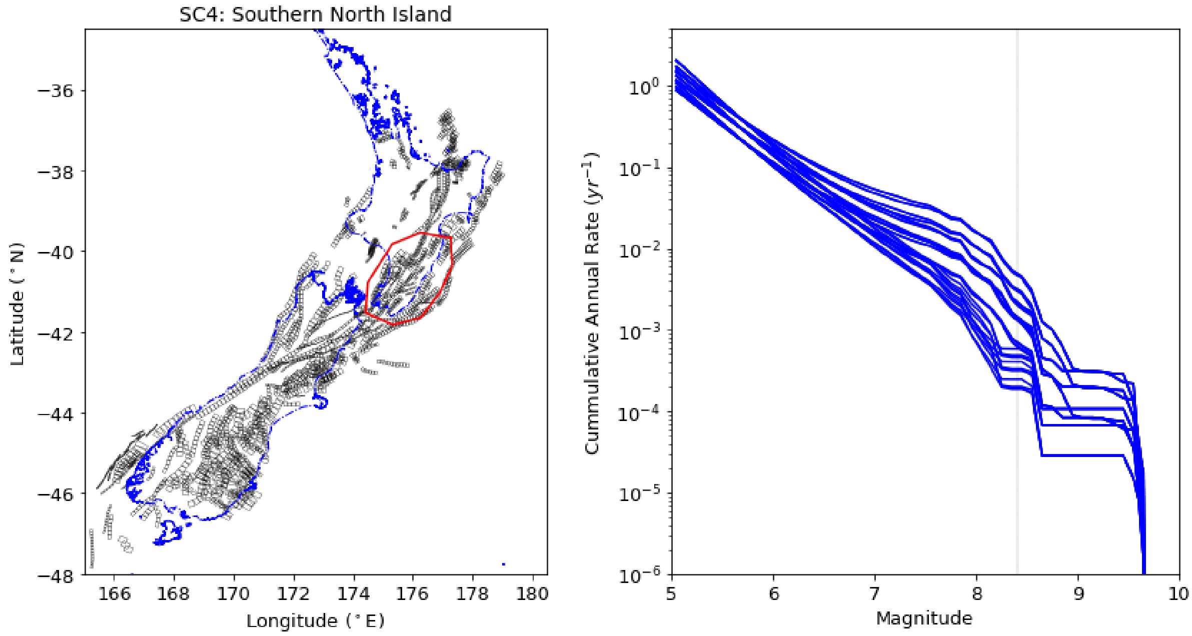

Figure A3.4 Scenario 4: As in Figure A3.1.

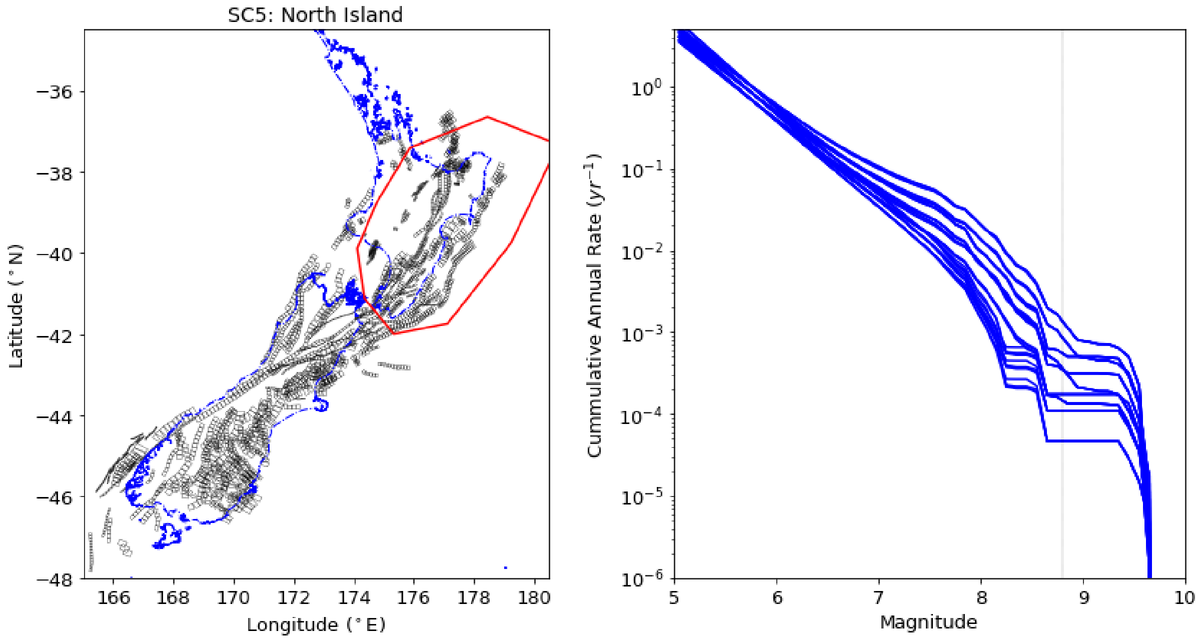

Figure A3.5 Scenario 5: As in Figure A3.1.

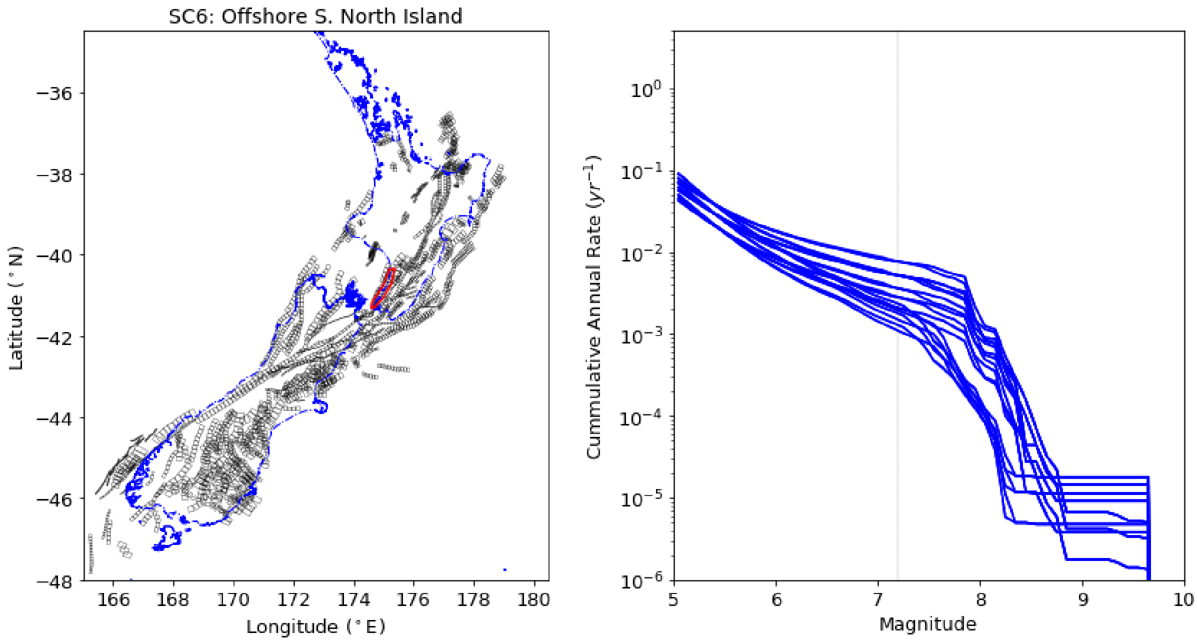

Figure A3.6 Scenario 6: As in Figure A3.1.

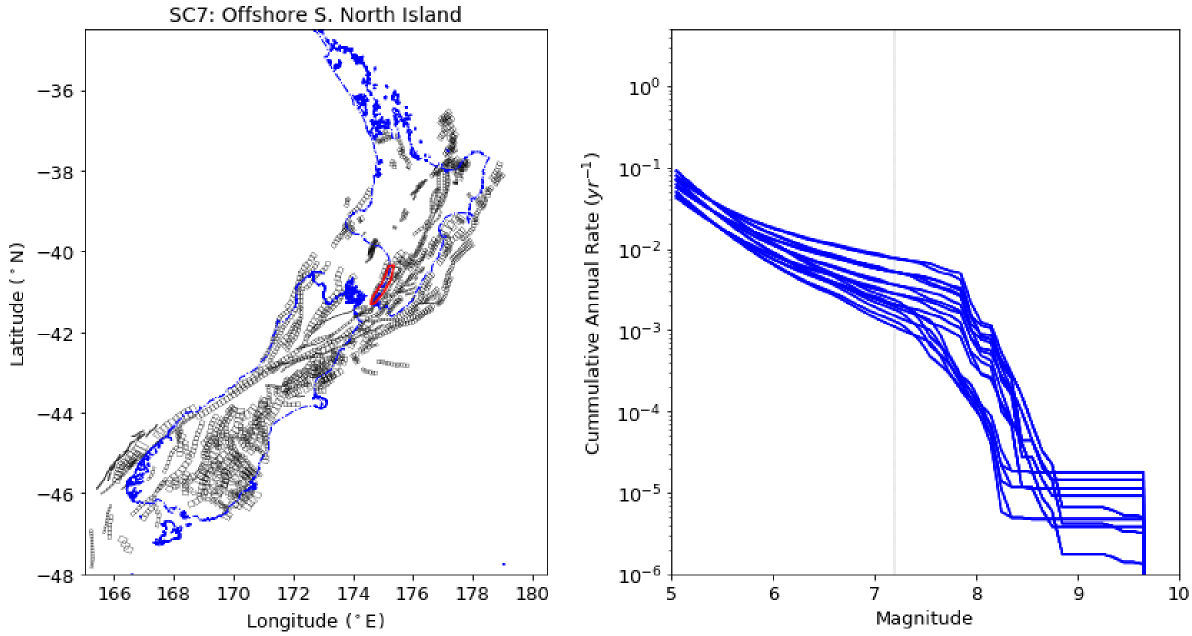

Figure A3.7 Scenario 7: As in Figure A3.1.

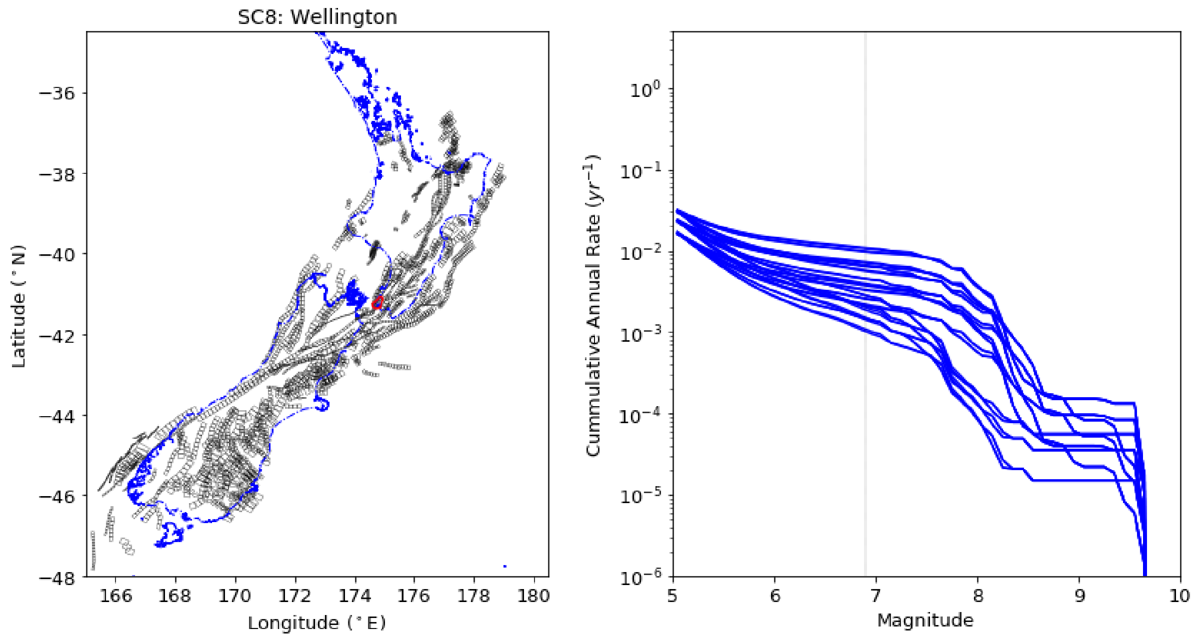

Figure A3.8 Scenario 8: As in Figure A3.1.

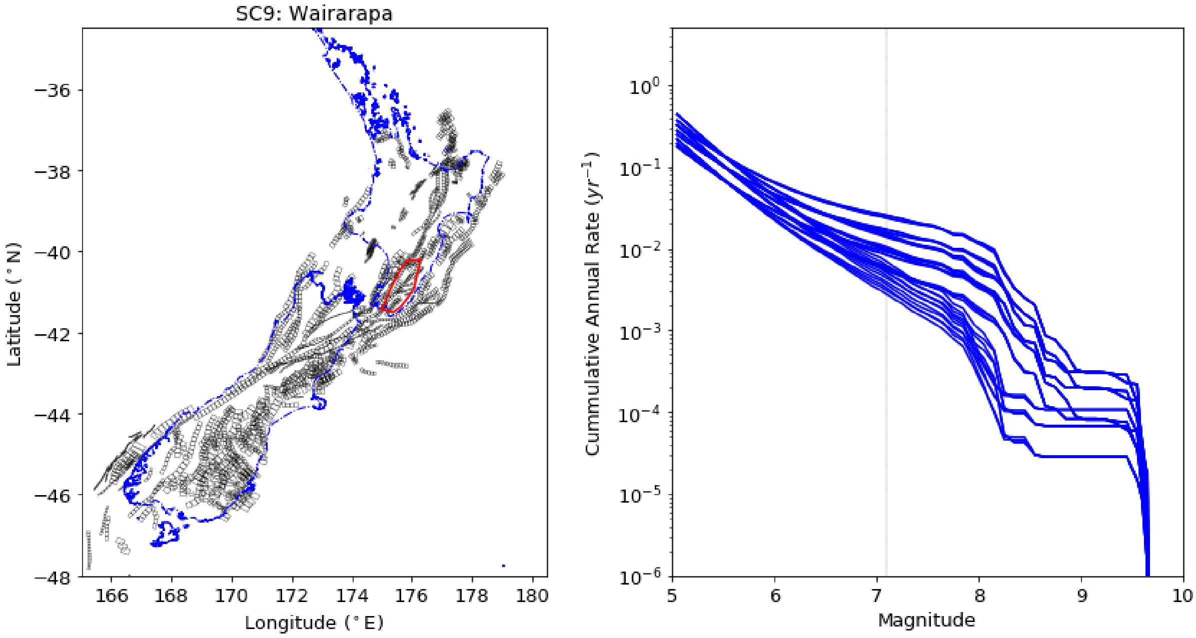

Figure A3.9 Scenario 9: As in Figure A3.1.

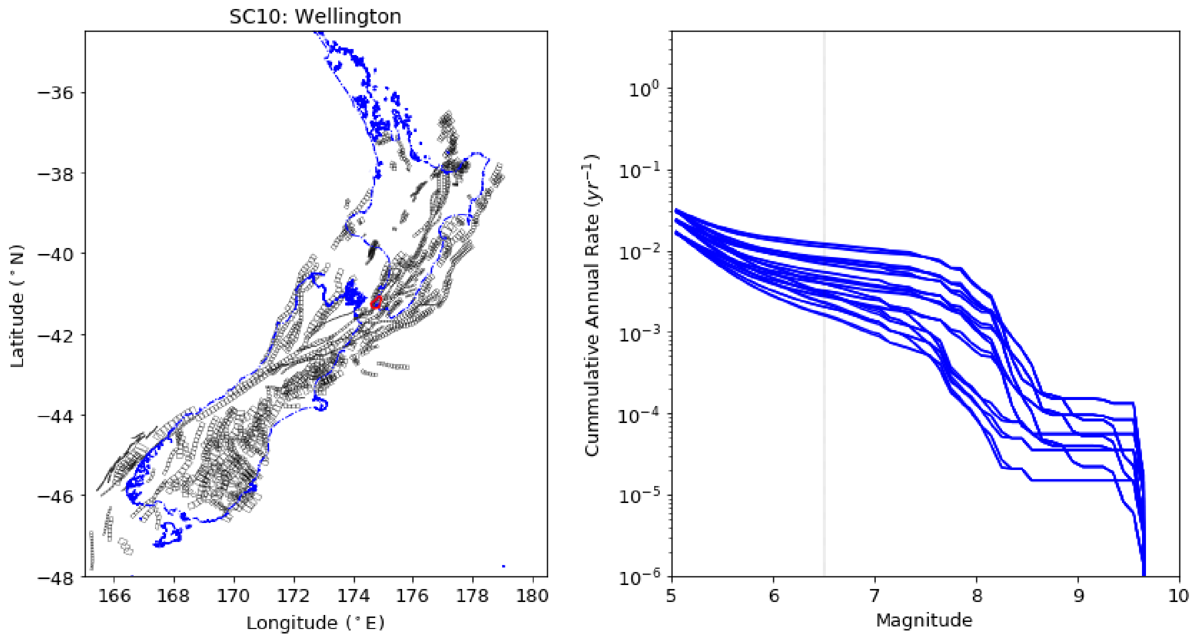

Figure A3.10 Scenario 10: As in Figure A3.1.

APPENDIX 4 GROUND-MOTION MODELS

Ground-motion models (GMM) were developed for each of the scenarios using the OpenQuake earthquake hazard and risk modelling tool developed by the Global Earthquake Model (Pagani et al. 2014). OpenQuake was configured with New-Zealand-specific models. The rupture models for the earthquake scenarios were prepared from RQSIM and converted into OpenQuake input rupture formats.

A4.1 Ground-Motion Models

A logic tree of multiple GMMs was used, which were developed and used in the 2022 National Seismic Hazard Model (Gerstenberger et al. 2022a). The GMM logic tree consists of 21 GMMs for crustal-fault sources and 12 GMMs for subduction interface models. OpenQuake requires one GMM logic tree to be used for a given scenario, so where the scenario had a combination of subduction interface and crustal sources, subduction interface GMM were used. For each scenario, 1000 ground-motion field realisations were generated for each GMM. This resulted in 21,000 ground-motion simulations for each crustal-fault source scenario and 12,000 ground-motion simulations for each subduction interface scenario. For each scenario, the mean and 84th percentile ground motions were then extracted from the suite of simulations for that scenario. The ground motion intensity metric type used for the simulations was peak ground acceleration (PGA).

A4.2 Site Parameter Model

To generate ground motions across New Zealand, a site parameter model is required that defines the soil type that amplifies or de-amplifies ground motions. For the GMMs used, the average shear wave velocity in the upper 30 m of soil (V_{s30}) is used as the site parameter. The New Zealand V_{s30} model of Perrin et al. (2015) was used.

A4.3 Ground-Motion Intensity

A ground motion to intensity conversion equation (GMICE) is required to convert PGA to MMI intensity. The GMICE of Moratalla et al. (2021) was used. This allows the results to be communicated in both PGA and MMI intensity. These two intensity metrics can then be linked to likelihood of damage using risk modelling.

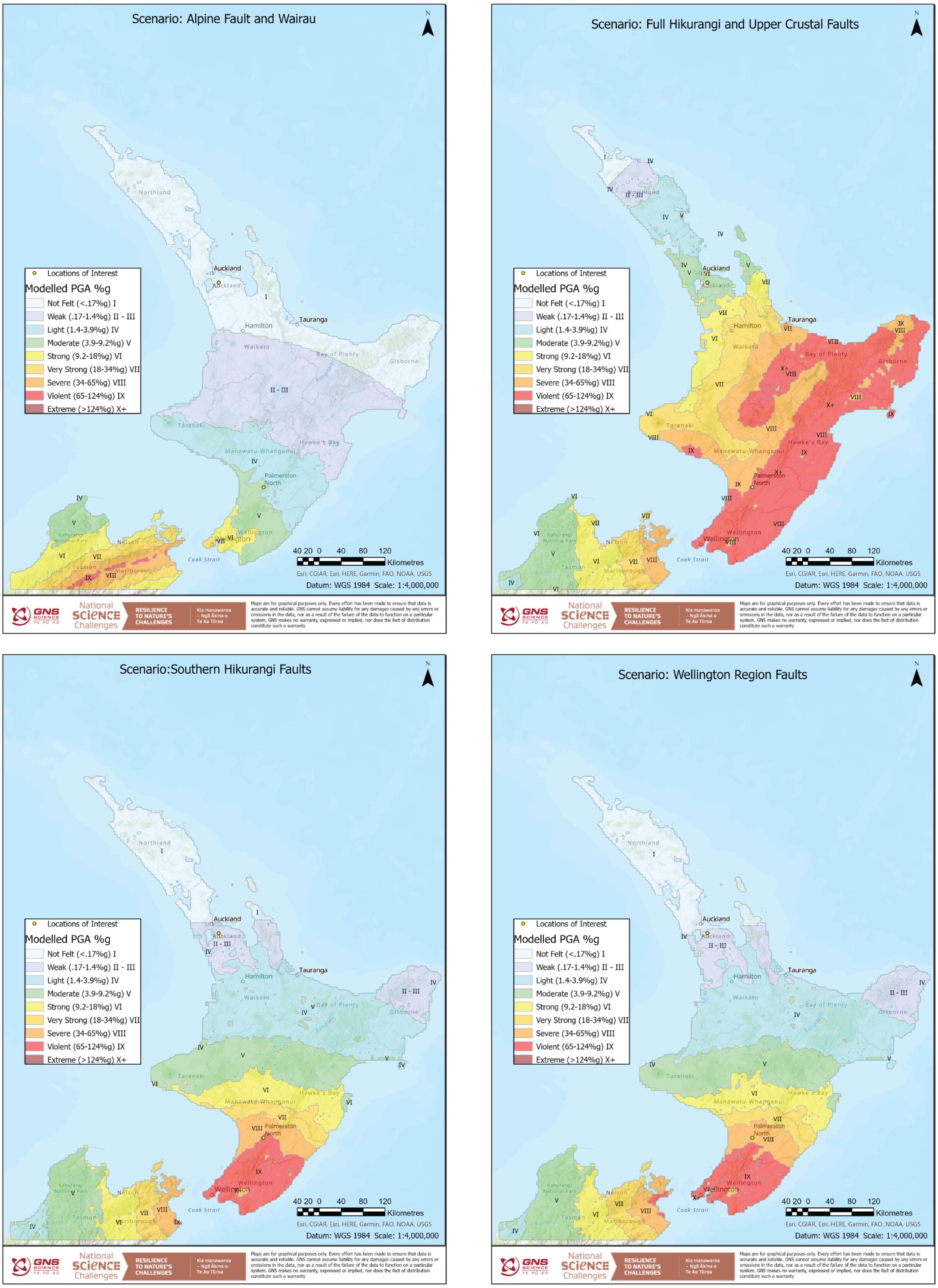

Figure A4.1 Spatial distributions of ground motions calculated for scenarios described in the text.

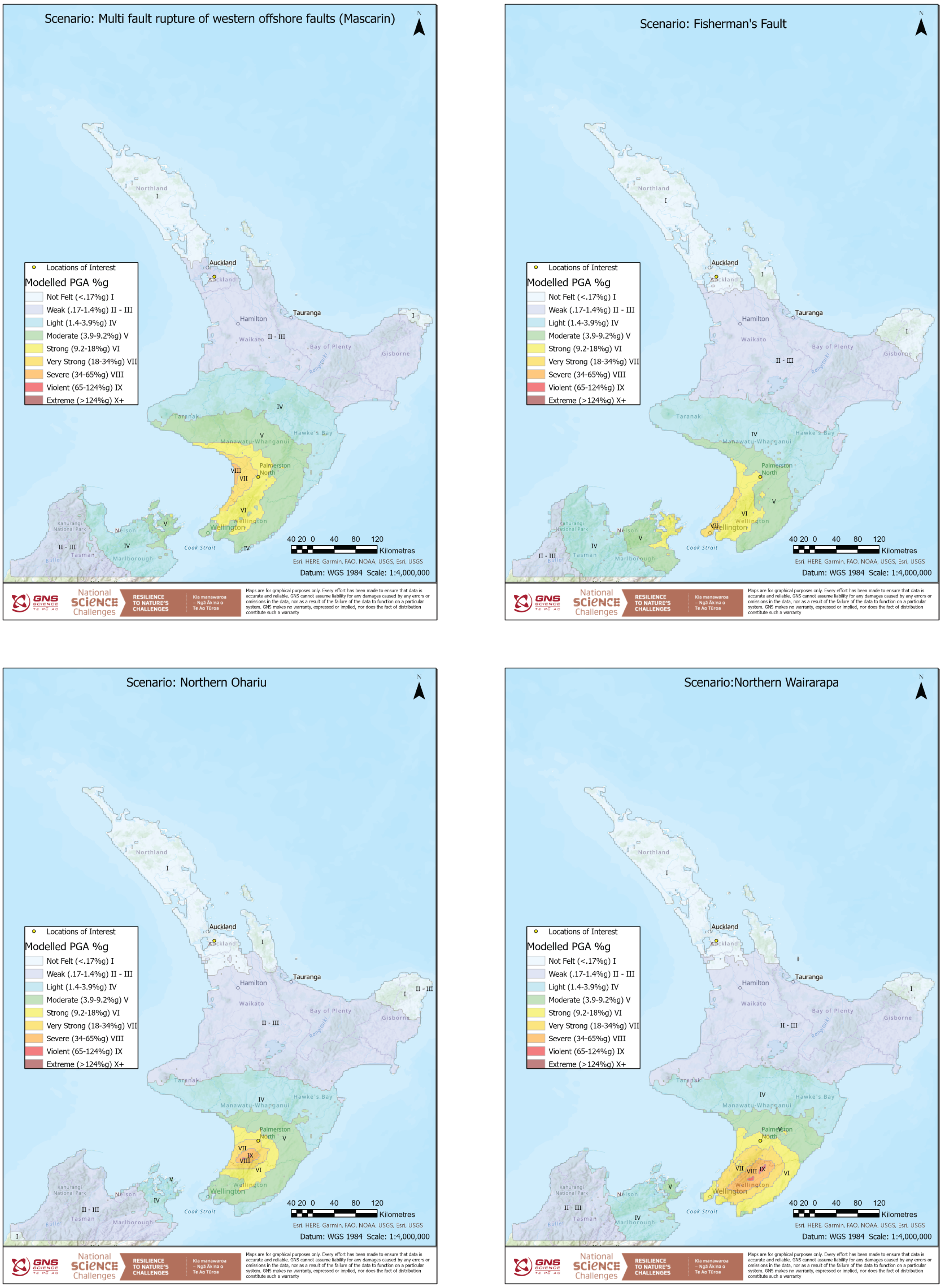

Figure A4.1 Continued. Spatial distributions of ground motions calculated for scenarios described in the text.

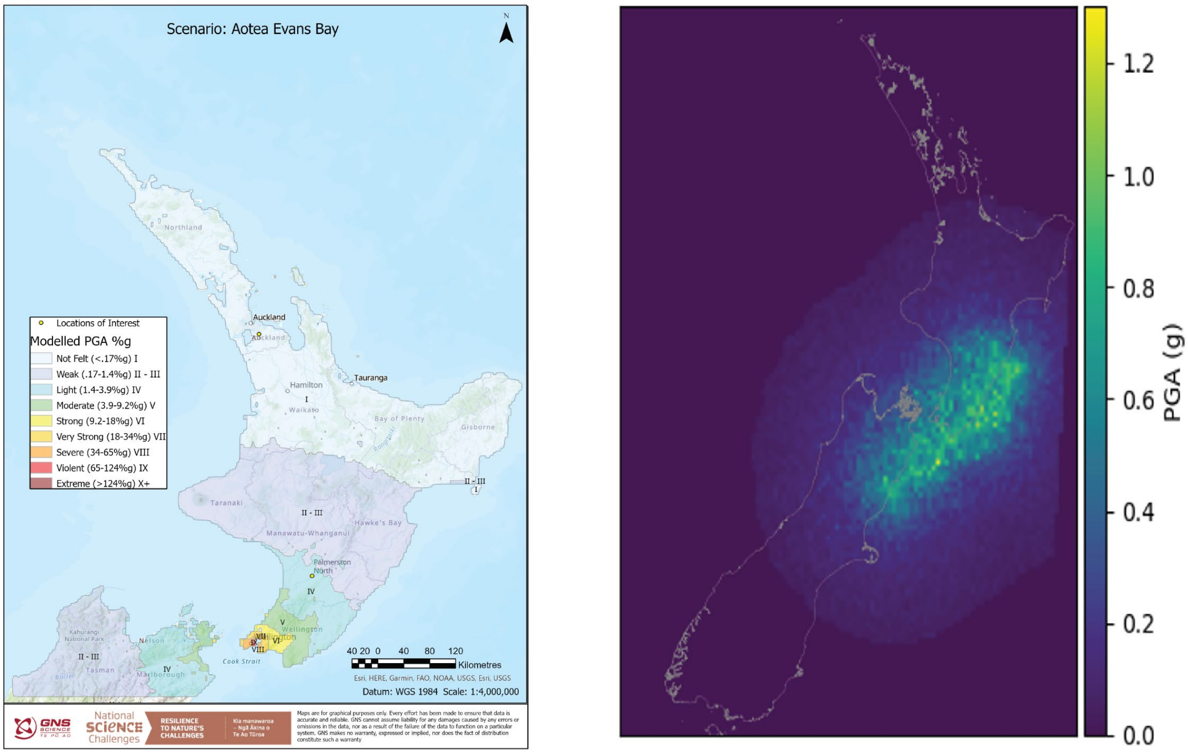

Figure A4.1 Continued. Spatial distributions of ground motions calculated for scenarios described in the text.

APPENDIX 5 LANDSLIDE HAZARD ASSESSMENT

A5.1 Landslide Probability

A5.1.1 Introduction and Aim

The aim of this component of the work was to quantify the relative landslide hazard from the given earthquake ground shaking at each of the three regional centres: Auckland, Palmerston North and Wellington.

Given the time constraints of this work, only the earthquake-induced landslide (EIL) susceptibility could be analysed. Landslide susceptibility is defined as a quantitative or qualitative assessment of the volume (or area) and spatial distribution of landslides, which exist or potentially may occur in an area. For this study, we have produced maps showing the subdivision of the terrain in zones (areas) that have a different probability that landslides of a given type may occur. The landslide types analysed here are predominantly debris and rock avalanches, which tend to be the more mobile types of landslides that occur during earthquakes (Massey et al. 2020). We do not include any analysis of potential landslide mobility/runout – defined as the probability that a specified landslide will reach a certain distance downslope or affect a specified area.

The landslide hazard intensity – defined as a set of spatially distributed parameters related to the destructive potential of a landslide – was then estimated using the EIL probability models from each earthquake simulation for each regional centre. These are then compared to the landslide hazard intensity from other well-documented earthquakes in New Zealand to compare the relative impacts of EIL potentially generated by each earthquake simulation.

For definitions of the terms used here, and other related landslide terms, please refer to de Vilder and Massey (2020).

A5.1.2 Methods

To estimate the landslide probability for each of the given earthquakes, we used a modified version of the EIL forecast tool described in Massey et al. (2021). The modification of the tool is described in Section A4.1.5. The model estimates the landslide probability from 0 to 1, where 1 = landslide occurrence at the regional scale, where ‘regional scale’ is defined as being 1:25,000 to 1:250,000 (Corominas et al. 2015). The algorithm underpinning the EIL forecast tool is a logistic regression model, which is a machine-learning-based classification model. The model was trained and tested on EIL distributions generated by the M_W 7.8 2016 Kaikōura, M_W 7.1 1969 Inangahua and M_W 7.3 1929 Murchison earthquakes.

The variables used in the model to forecast EIL probability are, in order of importance: Peak Ground Acceleration (PGA) as the forcing variable; and geology, slope, local slope relief, elevation and curvature as the susceptibility variables.

The landslide hazard intensity for each regional centre was calculated using the following steps:

- **Step 1:** The landslide probability forecasts were calculated with the modified logistic regression model using the PGA models derived from each of the 10 earthquake simulations across the full spatial extents of each PGA model. These were initially calculated using a 32 x 32 m grid cell resolution, which were then aggregated to 256 x 256 m and 512 x 512 m grid cell resolutions to aid visualisation of the results.

- **Step 2:** The EIL probabilities (at 32 x 32 m resolution) from each earthquake simulation were then sampled from within each regional centre and summed to calculate the total summed probability, which is a measure of the number of grid cells classified as being potential landslides.
- **Step 3:** The summed probabilities were then divided by the total number of grid cells within each regional centre to calculate a landslide density (%) for each earthquake simulation within each region.
- **Step 4:** The equivalent landslide densities were also calculated from the Kaikōura, Inangahua and Murchison earthquakes, as these represent large historical earthquakes that have triggered landslides that have both killed people and caused widespread devastation of the main areas affected. These historical EIL landslide densities were calculated for landslides within the 0.2 g PGA extent, which corresponds to the extent of the training areas used in the logistic regression modelling.

A5.1.3 Results

Maps showing the maximum landslide probabilities – the maximum probability from all nine of the earthquake simulations – for each region are shown in Figures A4.1–A4.3. These show that Wellington Region has the highest number of high-probability grid cells, with Auckland Region having the least.

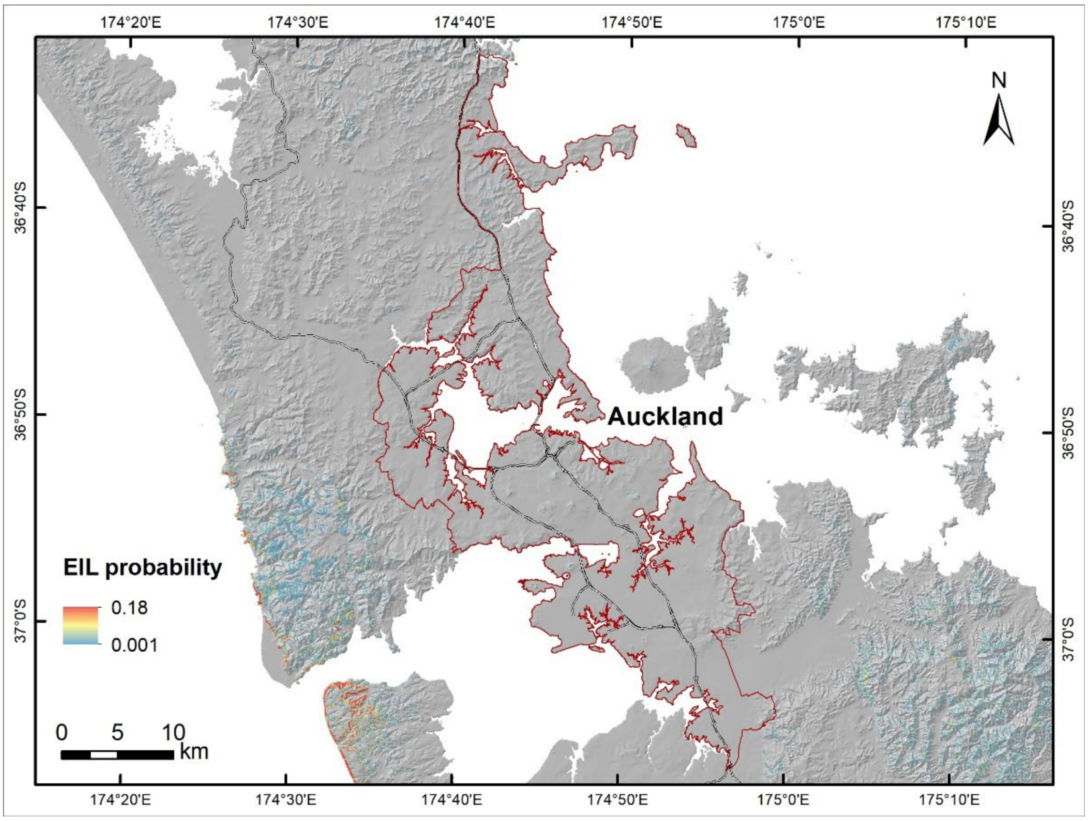

Figure A4.2 Earthquake-induced landslide (EIL) probability for the Auckland study area. The probabilities are the maximum values of all nine simulated earthquakes. The resolution of the model is 32 by 32 m, but the ground-motion models are at a resolution of 5 x 5 km. The main roads are shown and are taken from Land Information New Zealand (LINZ).

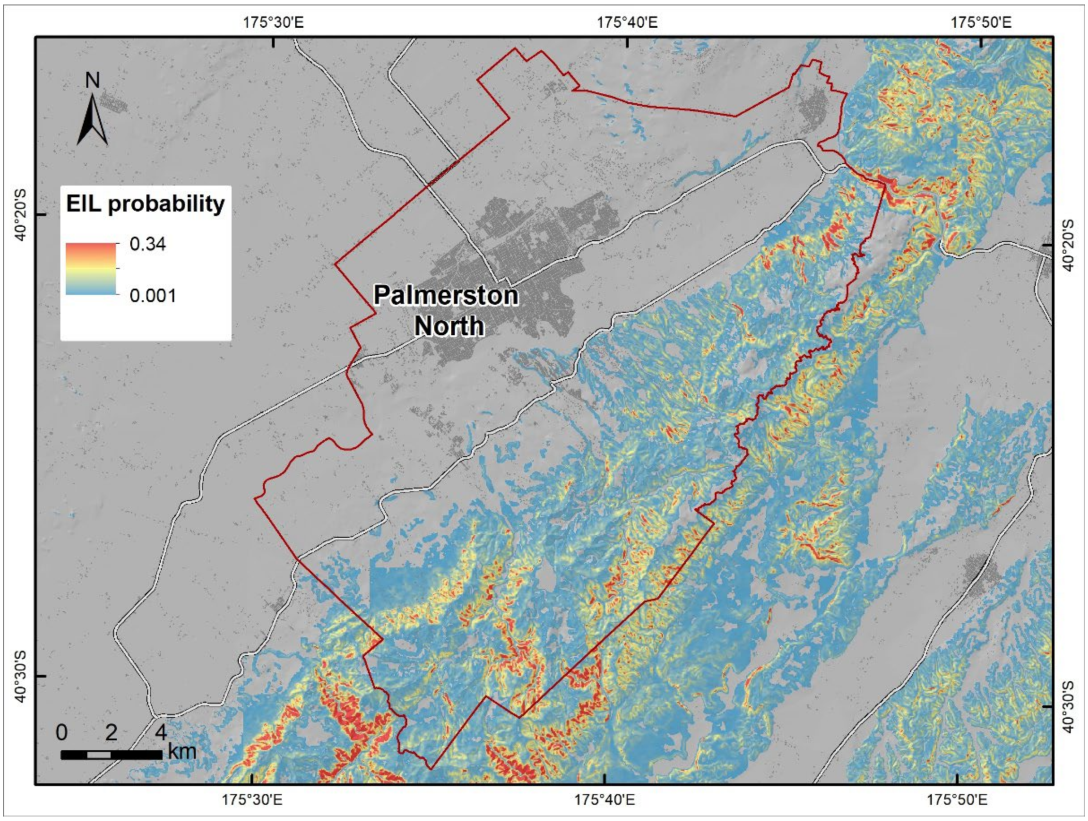

Figure A4.3 Earthquake-induced landslide (EIL) probability for the Palmerston North study area. The probabilities are the maximum values of all nine simulated earthquakes. The resolution of the model is 32 x 32 m, but the ground-motion models are at a resolution of 5 x 5 km. The main roads are shown and are taken from LINZ.

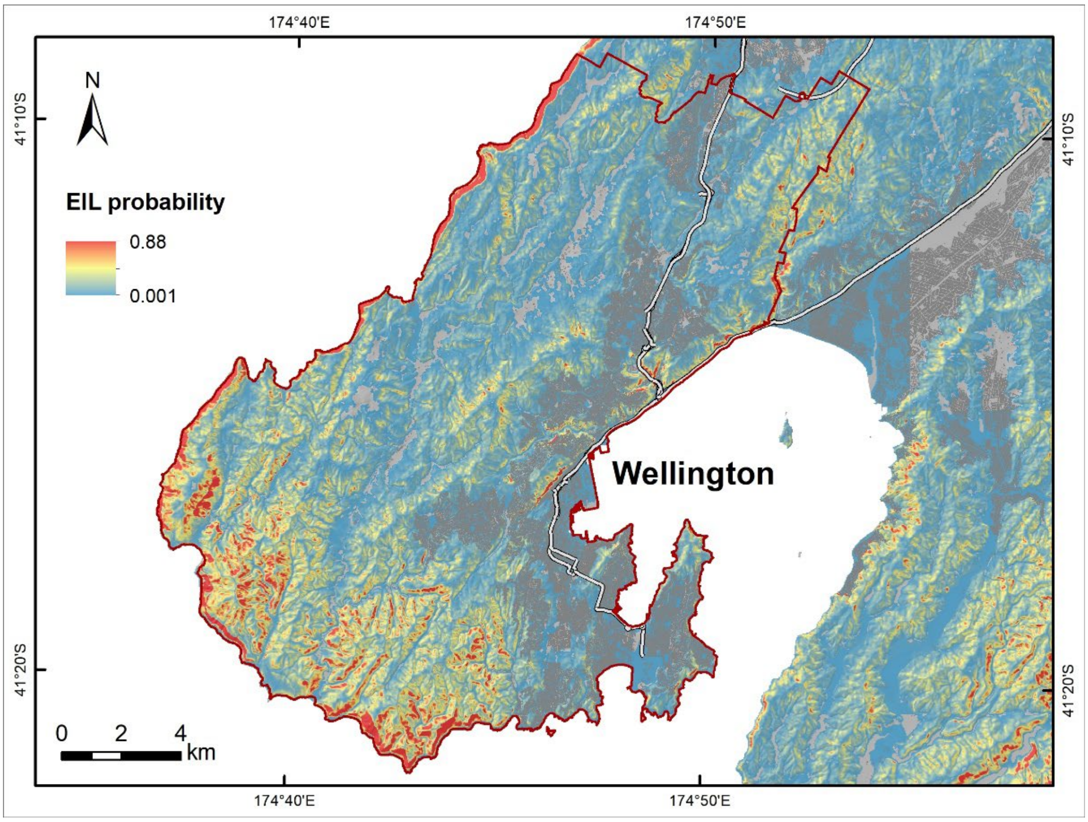

Figure A4.4 Earthquake-induced landslide (EIL) probability for the Wellington study area. The probabilities are the maximum values of all nine simulated earthquakes. The resolution of the model is 32 x 32 m, but the ground-motion models are at a resolution of 5 x 5 km. The main roads are shown and are taken from LINZ.

Figure A4.5 and Table A4.1 show the results for each study area plotted as landslide density per earthquake simulation. The average historical landslide density is calculated from the M_W 7.8 2016 Kaikōura, M_W 7.1 1969 Inangahua and M_W 7.3 1929 Murchison earthquakes. The historical landslide density is shown for comparison purposes, as these earthquakes generated many landslides over a wide region and caused widespread disruption to people and infrastructure in those regions.

Table A4.1 Landside density per earthquake scenario. The average historical landslide density is calculated from the overall landslide density recorded in three large historical earthquakes, the M_W 7.8 2016 Kaikōura earthquake, the M_W 7.1 1969 Inangahua earthquake and the M_W 7.3 1929 Murchison earthquake. Shading represents qualitative severity, with more severe impacts being shown in warm colours.

Earthquake Scenario	Landslide Density (within the 0.2 g PGA Extent?)			
	Auckland	Palmerston North	Wellington	Historical
rqs759464	0.1%	0.4%	0.7%	0.6%
rqs1237478	0.1%	0.2%	0.2%	-
rqs19118	0.1%	0.2%	0.2%	-
rqs37817	0.1%	0.2%	0.3%	-
rqs292713	0.1%	0.3%	0.7%	-
rqs1844079	0.1%	0.2%	0.2%	-
rqs1002623	0.1%	0.3%	0.8%	-
rqs950175	0.1%	0.2%	0.2%	-
rqs1010458	0.1%	0.2%	0.2%	-

Overall, the results (Figures A4.1–A4.4) show that the landslide densities for the Wellington study area are highest, followed by Palmerston North and then Auckland. The landslide densities for Auckland are all low and geographically located towards the west in areas that are sparsely populated. Conversely, the landslide densities for Wellington are highest and occur within the urban area and along the main transport routes in and out of the city. The landslide densities for three of the earthquake simulations exceed those caused by the historical earthquakes within their respective 0.2 g PGA extents. Although not in the study area, the Lower Hutt suburb of Eastbourne appears to have a relatively high number of high-landslide-probability grid cells. Of note in the Palmerston North study area is the Manawatū Gorge along the route of the now re-aligned State Highway 3. This area has a relatively high number of high-landslide-probability grid cells, indicating that, although non-earthquake-induced landslides were the reason for its re-alignment, EIL could have also caused significant issues and may even block the gorge, leading to landslide dams.

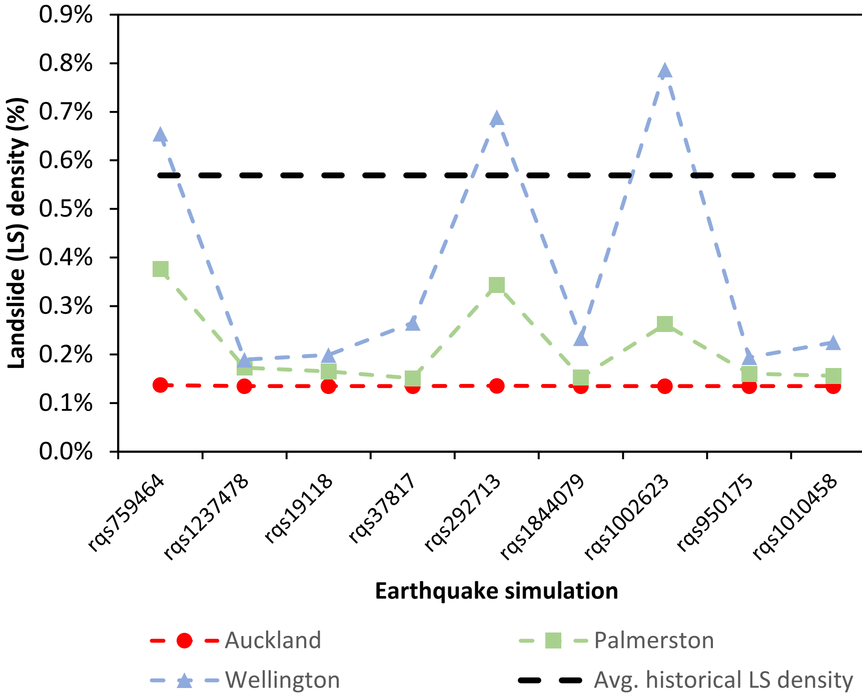

Figure A4.5 Landslide density plotted for each region for each earthquake. The average historical landslide density ('Avg. historical LS density') is calculated from the overall landslide density recorded in three large historical earthquakes, the MW 7.8 2016 Kaikōura earthquake, the M_W 7.1 1969 Inangahua earthquake and the M_W 7.3 1929 Murchison earthquake.

A5.1.4 Limitations

- Landslide runout is not considered in the landslide susceptibility models. This means that some areas of ground downslope of areas of high landslide susceptibility (probability) could be inundated by falling debris.
- Cumulative hazard along linear infrastructure has not been considered.
- Time-varying 'dynamic' landslide hazard has not been considered, meaning that, after a major earthquake, non-seismic landslide occurrence tends to increase and then decay with time after the major earthquake (e.g. Massey et al. 2022).

A5.1.5 Earthquake-Induced Landslide Model

The logistic regression model described in Massey et al. (2021) was modified by removing the fault distance ('FaultDist') forcing variable. This variable was defined as the Euclidean distance from the centroid of each of the 32 m sample grid cells to the nearest fault that ruptured using the mapped surface expression, taken from the GNS Science Active Faults database (Langridge et al. 2016), which includes those faults that ruptured during each earthquake.

The 'FaultDist' variable is included in the V2.0 forecast tool, which forecasts landslide occurrence immediately after an earthquake, when we do not know which faults have ruptured. When we run the EIL forecast tool straight after an earthquake, the tool only uses a PGA model based on an interpolation of the PGAs measured by the strong-motion instruments (with no fault models) along with all active faults within the 0.2 g PGA calculation window. These two variables are used to represent the earthquake forcing in the minutes after the occurrence of a major earthquake. The simulated earthquakes and the associated models of PGA used for this current work already include the rupturing faults, or subduction zone, as the earthquake source; therefore, the 'FaultDist' forcing variable was not required in the model.

For this work, we re-trained the logistic regression model without FaultDist but included all of the other variables as per those listed in Massey et al. (2021). This changed the relative weight of the other variables and resulting model coefficients. Validation of the model results was done using bootstrapping (Efron and Tibshirani 1994), which allowed the variability of the parameter values for each variable to be estimated within each GeolCode group. Bootstrapping is a way to assess the robustness of the parameter estimates derived from model fitting. For example, a robust estimate of the parameter for a given variable should have a narrow variation between the minimum and maximum and standard deviation either side of the mean, with a skewness – a measure of symmetry – between -1 and 1. Conversely, a poor estimate would be one with a wider variation.

To do this, we repeatedly drew random samples from the respective landslide datasets within each GeolCode and designated 20% of each random sample as the testing sample. The remaining 80% of the data from each sample was then used to fit a model, and the results were compared against the testing sample. A random sample was drawn 50 times, logistic regression models were fitted and the result statistics were calculated – minimum, maximum, mean and standard deviation of each variable parameter. Each of the 50 bootstrap logistic regression models were then applied to the entire dataset to calculate landslide probability and the specificity, sensitivity and area under the receiver operating characteristic (ROC:AUC) curve (Massey et al. 2021).

The results are shown in Tables A4.2–A4.7. These show that the coefficients for all variables within each GeolCode are robust, as they have a narrow variation between the minimum and maximum estimates, are normally distributed and are not skewed (all values are between -1 and 1).

Based on the ROC:AUC results (Table A4.7), the logistic regression models can be classified as ‘good’ to ‘excellent’ in their ability to forecast landslide probability for the three EIL inventories using the input variables listed. Overall, the results in Tables A4.2–A4.7 show that the statistical models developed here provide a robust forecast of landslide probability at different levels of earthquake PGA. However, the results from the models have a low pseudo R2, indicating that they cannot give accurate forecasts for individual grid cells. They may nevertheless give good overall estimates of the scale ‘intensity’ of landslide occurrence to be expected in individual earthquakes.

Table A4.2 GeolCode1 (Quaternary sands, silts and gravels): Logistic regression coefficients for the different variables used in the model derived from bootstrapping.

Variable Coefficient	Intercept	Elevation	Slope	Local Slope Relief	Curvature	PGA
Minimum	-10.10	-0.0010	0.03	0.06	-0.23	2.64
Maximum	-9.93	-0.0008	0.04	0.07	-0.16	2.79
Mean	-10.00	-0.0009	0.03	0.06	-0.20	2.70
Std. Dev.	0.04	0.00002	0.00	0.00	0.01	0.03
Skew	-0.22	0.6448	-0.34	0.27	0.80	0.11

Table A4.3 GeolCode2 (Neogene limestones, sandstones and siltstones): Logistic regression coefficients for the different variables used in the model derived from bootstrapping.

Variable Coefficient	Intercept	Elevation	Slope	Local Slope Relief	Curvature	PGA
Minimum	-10.03	0.0017	0.05	0.02	-0.11	2.39
Maximum	-9.89	0.0017	0.06	0.02	-0.09	2.46
Mean	-9.97	0.0017	0.05	0.02	-0.10	2.44
Std. Dev.	0.03	0.00002	0.00	0.00	0.01	0.02
Skew	0.55	0.2733	-1.02	-0.04	-0.36	-0.56

Table A4.4 GeolCode3 (Upper Cretaceous to Paleogene rocks, including limestones, sandstones, siltstones): Logistic regression coefficients for the different variables used in the model derived from bootstrapping.

Variable Coefficient	Intercept	Elevation	Slope	Local Slope Relief	Curvature	PGA
Minimum	-8.42	-0.0003	0.03	0.02	-0.14	2.15
Maximum	-8.29	-0.0002	0.04	0.03	-0.12	2.22
Mean	-8.35	-0.0003	0.03	0.03	-0.13	2.19
Std. Dev.	0.03	0.00003	0.00	0.00	0.01	0.02
Skew	0.09	-0.2147	-0.21	0.54	-0.66	-0.11

Table A4.5 GeolCode4 (All intrusive and extrusive igneous rocks): Logistic regression coefficients for the different variables used in the model derived from bootstrapping.

Variable Coefficient	Intercept	Elevation	Slope	Local Slope Relief	Curvature	PGA
Minimum	-8.05	-0.0009	0.01	0.03	-0.16	1.94
Maximum	-7.82	-0.0007	0.01	0.03	-0.12	2.02
Mean	-7.94	-0.0008	0.01	0.03	-0.14	1.97
Std. Dev.	0.05	0.00003	0.00	0.00	0.01	0.02
Skew	0.33	0.1051	0.14	0.00	-0.33	0.09

Table A4.6 GeolCode5 (Lower Cretaceous Torlesse [Pahau terrane] ‘basement’ rocks): Logistic regression coefficients for the different variables used in the model derived from bootstrapping.

Variable Coefficient	Intercept	Elevation	Slope	Local Slope Relief	Curvature	PGA
Minimum	-8.05	-0.0009	0.01	0.03	-0.16	1.94
Maximum	-7.82	-0.0007	0.01	0.03	-0.12	2.02
Mean	-7.94	-0.0008	0.01	0.03	-0.14	1.97
Std. Dev.	0.05	0.00003	0.00	0.00	0.01	0.02
Skew	0.33	0.1051	0.14	0.00	-0.33	0.09

Table A4.7 Results from the model fitting: Calculated as the Nagelkerke (pseudo R^2) and area under the random operator characteristic curve (ROC: AUC).

GeolCode	Pseudo R^2	ROC:AUC
1	0.23	0.91
2	0.28	0.89
3	0.14	0.82
4	0.09	0.76
5	0.17	0.86

APPENDIX 6 TSUNAMI HAZARD ASSESSMENT

A6.1 Offshore Tsunami Hazard for Auckland and Wellington

The scope and timeframe of this report do not allow detailed tsunami inundation scenarios from each event. Rather, we have explored existing work to comment about the tsunami hazard. In 2021, GNS Science updated the National Tsunami Hazard Model (NTHM). The model estimates the maximum tsunami height within 20 km sections of coast at a range of different return periods (inverse of the annual probability of exceedance [Power et al. 2022]). Note that the NTHM estimates the probability of wave heights at the coastline, not onshore run-up values or inundation extents. Figure A5.1 shows the tsunami amplitudes around New Zealand at the 2500-year return period at the 84th percentile confidence interval. The Yellow Tsunami Evacuation Zones in New Zealand should be at least as large as the area inundated by tsunami at this return period and confidence level. For a structure as critical as the NCMC, in the opinion of GNS Science, this seems to also be a minimum appropriate design level for it as well. At this particular combination of return period and confidence, the overall tsunami hazard from all earthquake sources (local, regional and distant) is similar for the sections of coast to the east or west of Auckland (about 3–5 m), slightly lower on the western side. The tsunami hazard offshore Wellington is much higher and is approximately 10 m at this return period and confidence level.

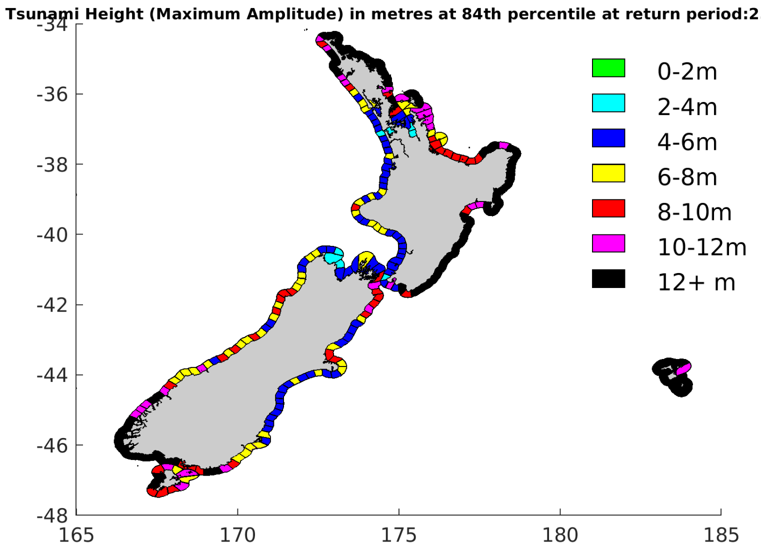

Figure A5.1 Expected maximum tsunami height in metres at the 2500-year return period, shown at 84th percentiles of epistemic uncertainty.

Figure A5.2 shows the hazard curves and deaggregation pie chart for the section of coast on Auckland City's east coast. The deaggregation is taken at the 50th percentile (median) of uncertainty at the 2500-year return period, not the 84th percentile used for the yellow zone, but it would likely be similar. The majority of the hazard comes from a large M_W 9 earthquake on the Kermadec Subduction Zone. However, other distant sources also contribute to the hazard for this region, notably Alaska and the Kuril subduction zones in the North Pacific. This means that those zones can produce similar size tsunami to that from the Kermadec subduction zone, but at a lower probability due to the higher magnitude required. The NTHM uses 'Effective Magnitudes', as it is based on modelling tsunami caused by earthquakes of uniform slip, and the effects of non-uniform slip are approximated by changes to the moment magnitude of the uniform slip events. This means that a similar-sized tsunami size could be possible from an earthquake with a lower seismic magnitude than that shown on the deaggregation, but which has a non-uniform slip distribution.

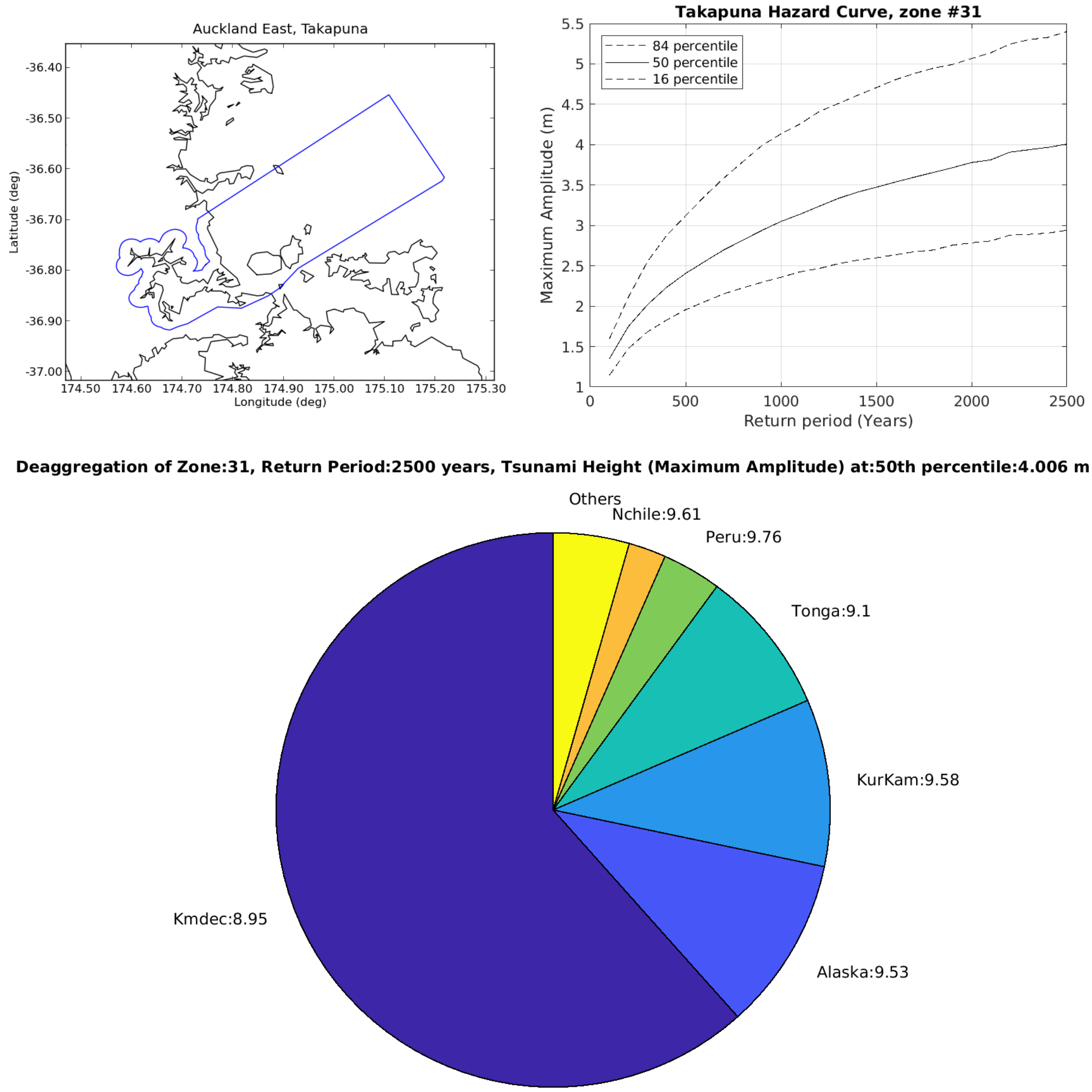

Figure A5.2 Area map, tsunami hazard curve and deaggregation pie chart at the 2500-year return period, median hazard value for the Auckland East coastal section.

Figure A5.3 shows the similar charts for the Auckland West section of coast. Tsunami hazard here is slightly lower than for the east coast. The Kermadec subduction zone is again the most significant source but from a higher-magnitude event. Unlike the east coast, the next most significant sources of hazard in the NTHM at this return period are from the Puysegur subduction zone southwest of New Zealand and the South Solomons subduction zone. Other more distant sources, such as the Alaskan subduction zone, again contribute to the hazard.

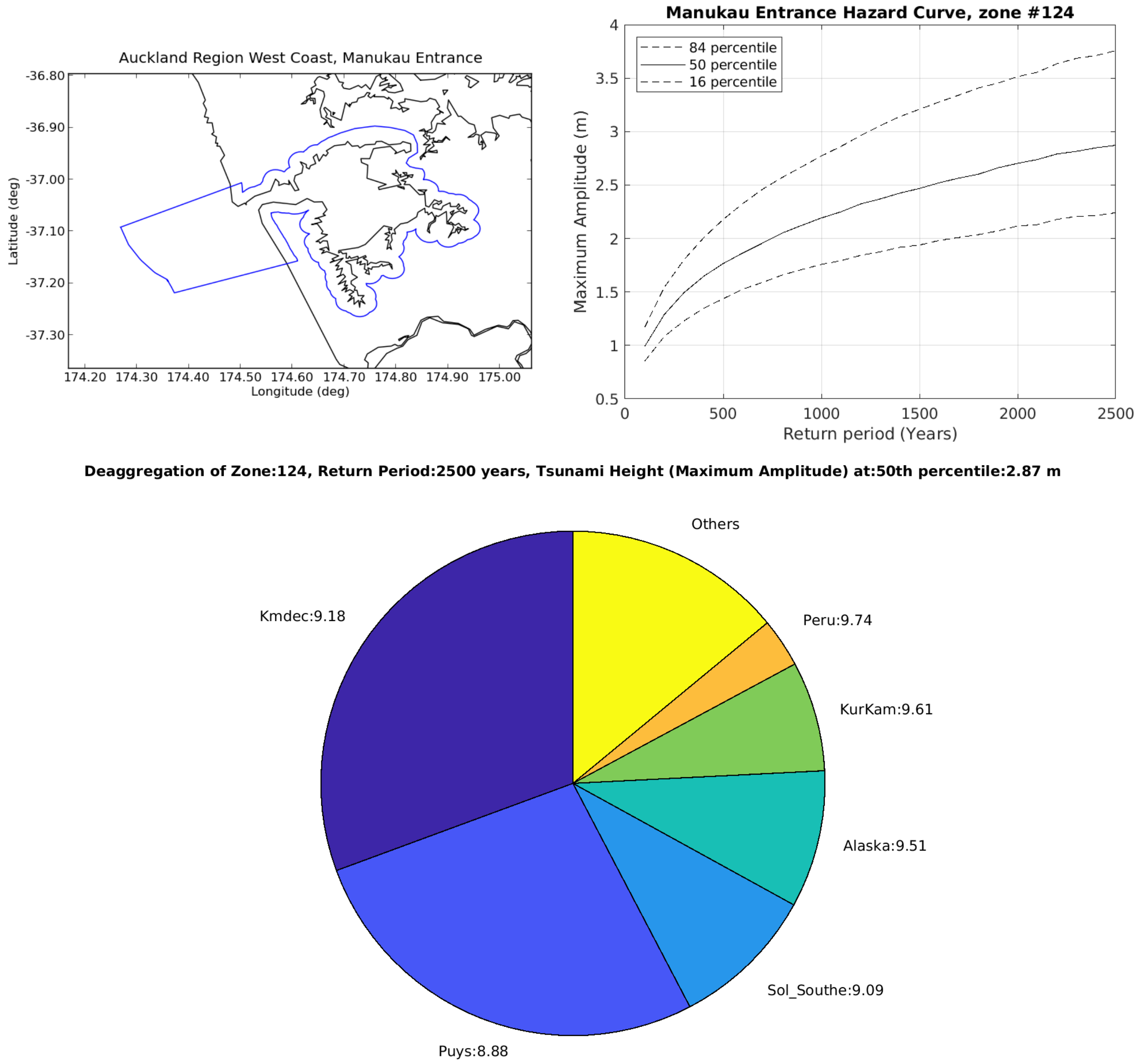

Figure A5.3 Area map, tsunami hazard curve and deaggregation pie chart at the 2500-year return period, median hazard value for the Auckland West coastal section.

Figure A5.4 shows the same set of figures for the Wellington Zone. Unlike Auckland, the local faults contribute much more to the hazard in this area, most particularly, the Hikurangi subduction zone. The tsunami hazard is overall much higher than for the previous two zones, more than double. Local crustal faults are also important components to the hazard in this area (e.g. the Jordon-Kekerengu-Needles Fault and the Wairarapa Fault).

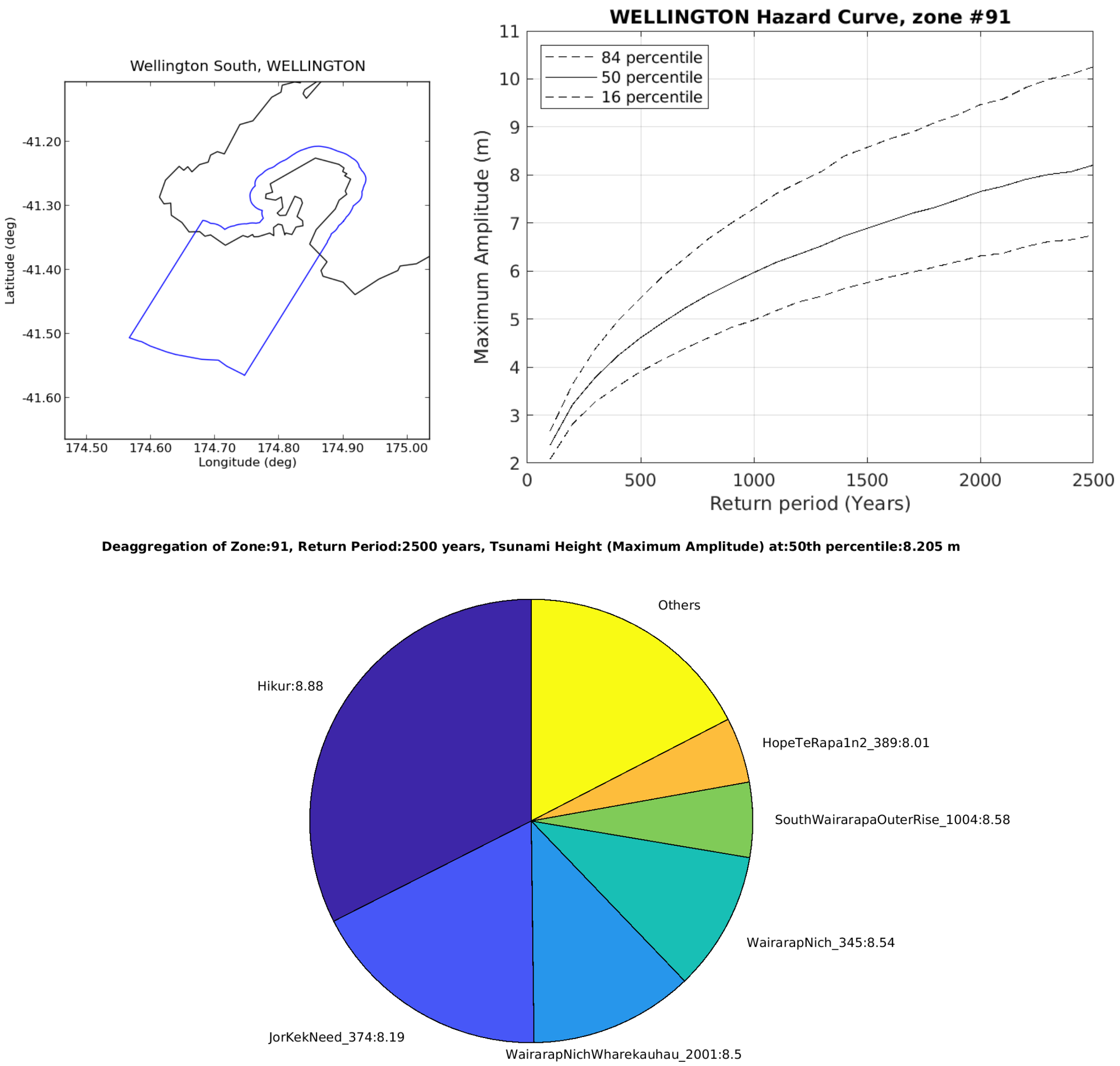

Figure A5.4 Area map, tsunami hazard curve and deaggregation pie chart at the 2500-year return period, median hazard value for the Wellington coastal section.

In addition to this work, GNS Science updated the tsunami scenario database that underpins both the NTHM and New Zealand's threat maps in 2019 (Gusman et al. 2019). The threat maps are figures showing the maximum tsunami amplitude expected across New Zealand's tsunami warning zones from the scenarios in the database. They are used early in a response to provide an initial estimate of the potential tsunami threat from regional or distant earthquake sources (i.e. those with more than one-hour travel time to New Zealand). From an inspection of the database, a very large (usually M9+, sometimes high magnitude 8) earthquake on several subduction zones around the Pacific would be large enough to cause an evacuation in both Wellington and Auckland simultaneously (i.e. an offshore wave height of 1 m or more in both zones). Some examples are shown in Figure A5.5, but there are other subduction zones for which this is true. The exact magnitude at which this occurs for a given subduction zone depends on details such as the location of the zone and the orientation of the plate boundary. As a guide, the Orange evacuation zones in Auckland or Wellington can be used as an estimate of the area that might be inundated by any of these very large, and rare, circum-Pacific earthquakes. The Orange Zone in New Zealand is usually based on the inundation from a 3 m or 5 m tsunami in a given region and would generally be large enough to cover the inundation from these types of sources. The exact area inundated by a given scenario would need to be determined by detailed numerical modelling and is beyond the scope of the current project.

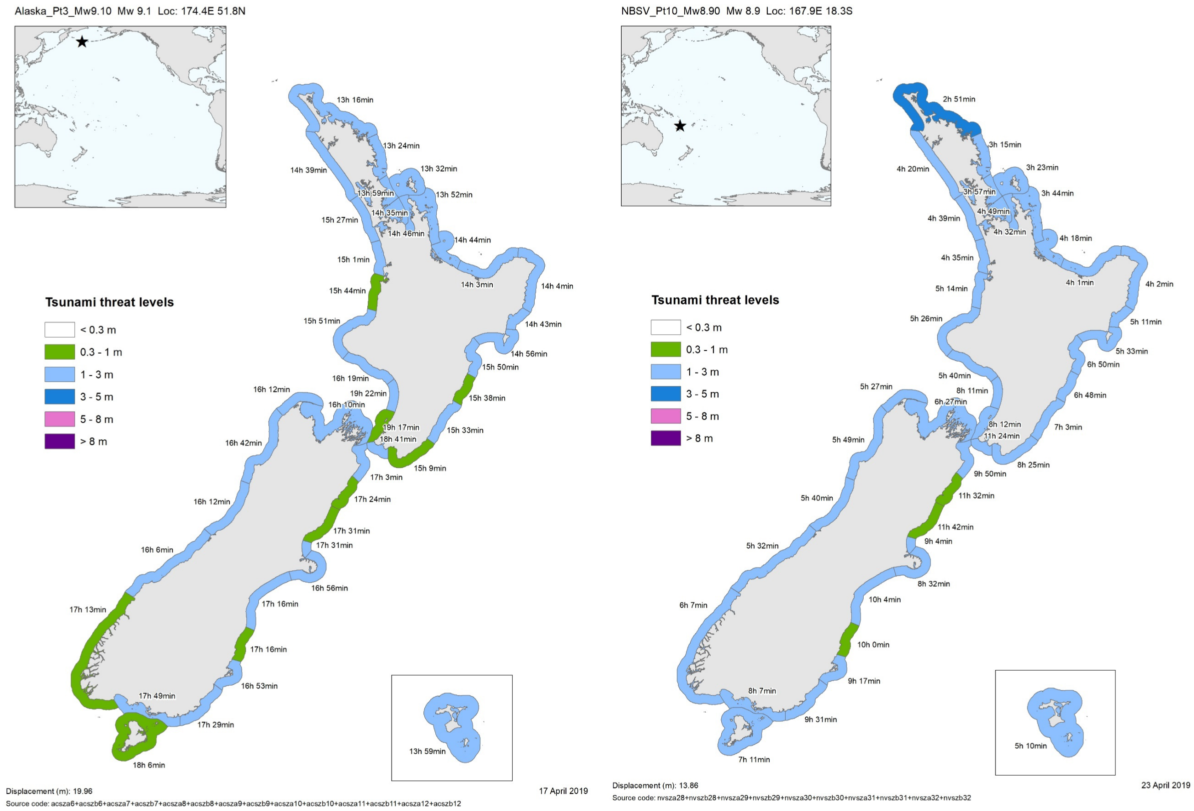

Figure A5.5 The tsunami threat map for a very large (Mw 8.9 or 9.1) uniform slip earthquake on the (a) Alaskan subduction zone or (b) South Solomon Zone, with the location of the centroid shown by the star. Both the Wellington and Auckland zones are estimated to experience offshore wave heights above 1 m. Also shown are the estimated times of first arrival at each zone. The maximum tsunami amplitude on which the threat map is based would arrive later.

A6.2 Tsunami Inundation Modelling for Auckland and Wellington

In terms of inundation modelling, GNS Science has not done any detailed tsunami inundation models for Auckland in recent times. GNS Science understands that eCoast has recently done some models in Auckland for Council to inform their evacuation zones, but these are not in the possession of GNS Science at the present time. Some older models were also done by NIWA for a probabilistic tsunami inundation study for Auckland.

As we do not have a recent inundation model for Auckland, one approach is to simply examine the 20 m elevation contour and the location of relevant assets. This should be suitable to screen for infrastructure where tsunami may be of concern. It is considered very unlikely that a tsunami from an earthquake source would inundate past the 20 m elevation contour in Auckland. This is done in Figure A5.6 for the Auckland region. The Auckland aNCMC sites are all well above this contour. However, the airport is within it. Given its location at the back of a shallow harbour on the west side of Auckland, the airport is only likely to be inundated if there was a very large earthquake on a subduction zone such as the Puysegur or Solomon Islands subduction zones. However, determining exactly what event would inundate the airport, and the damage it may cause and the extent of any resulting repair time, is beyond the scope of the current report.

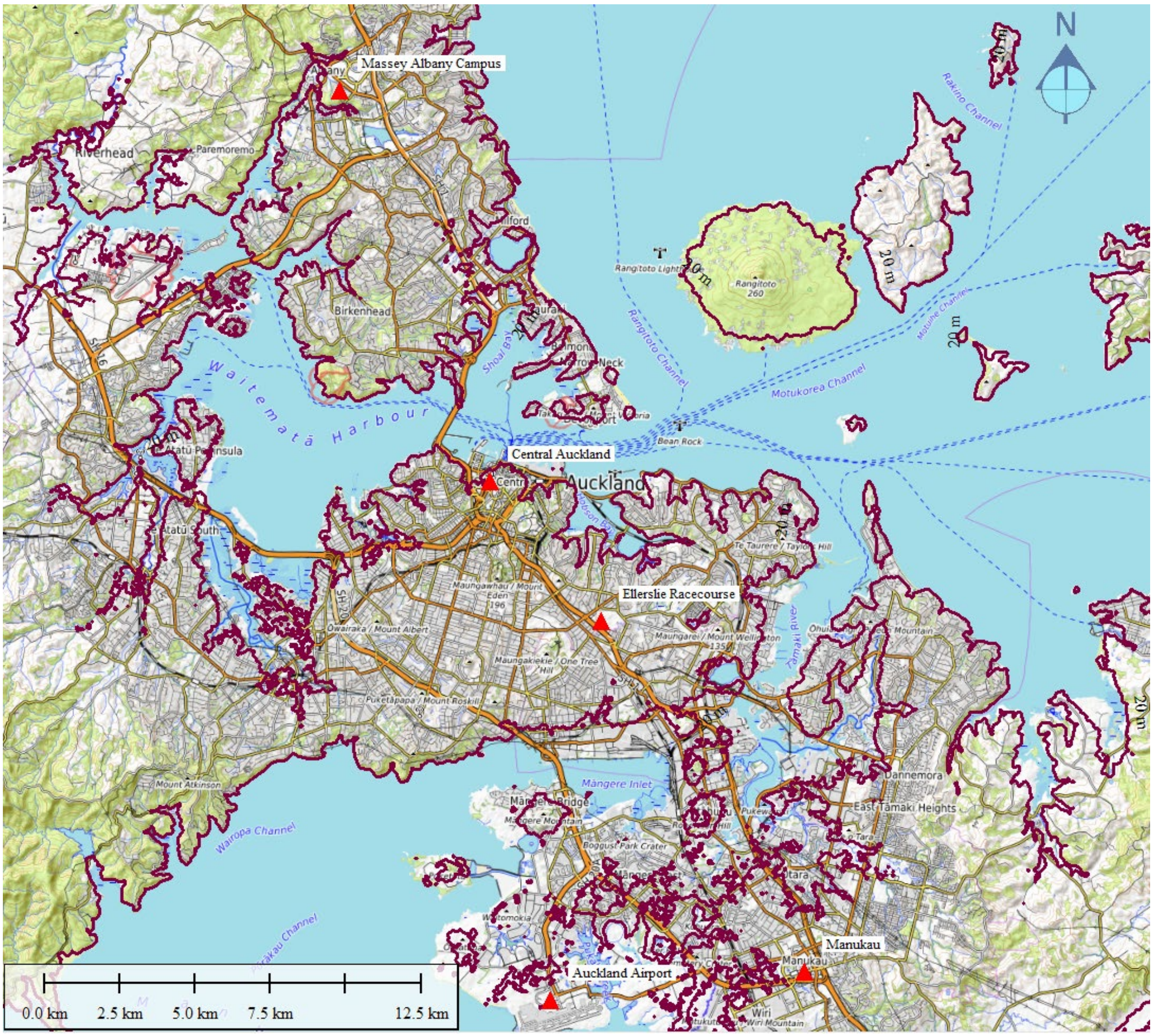

Figure A5.6 20 m elevation contour and the location of some possible locations of the aNCMC and critical infrastructure (red triangles). Of these, only the airport lies within the 20 m elevation contour.

For Wellington, GNS Science has done numerous tsunami inundation models for the area for the regional and city councils in projects such as the Blue Line project. For example, we modelled the tsunami caused by a Mw 8.9 earthquake for the Hikurangi Response Project (see Figure A5.7). Recently, GNS Science has also completed some work for Wellington City Council for their land-use planning. We can provide the maps to NEMA if required, although we would probably require agreement from the Council first as the funding party. We also would need agreement from NIWA, as the models in question use Wellington Harbour data provided to GNS Science by NIWA. Under the terms of our data-sharing agreement with NIWA, we cannot use the derived products for commercial projects such as this without permission of NIWA, and we may also be required to pay them a fee. Negotiating this for this project may be possible but is likely to take some time to arrange, beyond that available for the current phase of the project. However, we do not believe that any of these models would be of great help to this project. It would seem to us to be simpler, and adequate at this screening stage of the project, to just use the publicly available tsunami evacuation maps and/or elevation contours. The evacuation can be used to provide initial estimates of inundation extent for large local (Yellow Zone) or large regional and distant (Orange Zone) tsunami sources for screening purposes in both areas. Alternatively, just inspection of elevation contours can be used at this screening stage of the project, as described above. Another issue with the existing inundation models that we do have is that they do not use exactly the same earthquake sources as those from the synthetic catalogue, and none of them model the tsunami inundation in Wellington and Auckland with exactly the same scenario. If these are required for this project at a later date, it would likely to be more efficient to simply model bespoke scenarios for this project once the proposed site of the aNCMC has been further narrowed down.

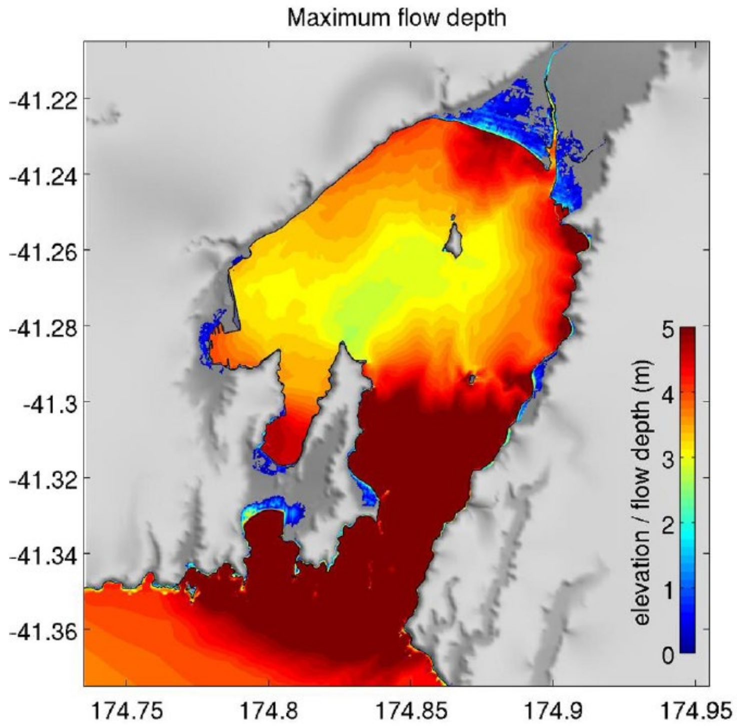

Figure A5.7 The maximum flow depth and offshore tsunami height for the Mw 8.9 Hikurangi Response Scenario. From Power et al. (2018).

A6.3 Derivation of the Tsunami Entries in the Hazards Summary Table

The tsunami entries in the Hazards Summary table (Figure 3.1) were populated qualitatively using expert opinion. This was done making the following assumptions:

- The Beehive basement was assumed to become unsafe to use once water from a tsunami reaches the ground floor of Bowen House.
- The remaining potential alternative NCMC sites in Manawatū are more than 10 km inland from the coast, and those in Auckland more than 20 m above sea level.
- The likelihood categories in the table were chosen considering the range of plausible ruptures on the named faults at the given magnitude. The specific slip distributions in Appendix 2 were viewed as just one example from this range.
- Seiching was considered, in the sense of resonant oscillations in a body of water. The direct 'splash' effect of coseismic horizontal translation at the shore was excluded.
- Where consensus was not achieved among the consulted experts, a (+) symbol indicates that one expert would have preferred a higher likelihood and a (-) symbol indicates that one expert would have preferred a lower likelihood.
- The 'Northern Wairarapa Fault' scenario was assumed to lie entirely on the onshore part of the Wairarapa Fault.
- For the 'Southern Hikurangi scenarios', it was assumed that plate interface rupture occurs only south of Hawkes Bay.

A6.4 Summary

In summary, Auckland has a much lower tsunami hazard than Wellington. For Auckland, the main sources of earthquake-generated tsunami hazard are regional and distant earthquake sources. On the east coast of Auckland, the Kermadec is a significant contributor to the tsunami hazard there. For Wellington, local sources, particularly the Hikurangi Subduction Zone, are the most important. If a very large earthquake (high magnitude 8 and above) were to occur in one of the circum-Pacific subduction zones, then both Auckland and Wellington may require evacuation simultaneously. Inundation is likely to be within the areas covered by their Orange Evacuation Zones in this case. The mostly likely source to create a very large and much more damaging tsunami to both areas is a very large Hikurangi / southern Kermadec earthquake (or sequence of earthquakes) that extends from Cook Strait to beyond East Cape, either in one large event or as a series of large events over a short period of time (weeks to years). This sort of event is covered earlier in this document. The possibility of a tsunami impacting both cities at once from any of these sources is thus very low but is not impossible. The possibility of a tsunami impacting both cities to an extent that the NCMCs in both cities become unusable is even lower, as the currently proposed sites in Auckland are above 20 m elevation. If an inland/elevated site is chosen for the alternative NCMC, then this possibility of having a tsunami impact both sites (and the infrastructure needed for their operation, such as airports) would be eliminated entirely. From a tsunami point of view, ignoring other perils, an inland/elevated location well way from the coast for the aNCMC is thus the safest possible option. A coastal option may also be acceptable from a tsunami point of view depending on the risk tolerance and specific proximity and elevation of the sites and supporting infrastructure compared to an inland option.

www.gns.cri.nz

Principal Location

1 Fairway Drive, Avalon
Lower Hutt 5010
PO Box 30368
Lower Hutt 5040
New Zealand
T +64-4-570 1444
F +64-4-570 4600

Other Locations

Dunedin Research Centre
764 Cumberland Street
Private Bag 1930
Dunedin 9054
New Zealand
T +64-3-477 4050
F +64-3-477 5232

Wairakei Research Centre
114 Karetoto Road
Private Bag 2000
Taupo 3352
New Zealand
T +64-7-374 8211
F +64-7-374 8199

National Isotope Centre
30 Gracefield Road
PO Box 30368
Lower Hutt 5040
New Zealand
T +64-4-570 1444
F +64-4-570 4657